UNIVERSIDADE D
COIMBRA

João Miguel Fernandes Vieira

CARBON NANOTUBE MODIFIED CARBON FIBER MICROELECTRODES FOR *IN VIVO* OXIMETRY IN AN ANIMAL MODEL OF TEMPORAL LOBE EPILEPSY

Dissertation submitted to Faculty of Sciences and Technology of the University of Coimbra for the Master's degree in Biomedical Engineering with the specialization in Neurosciences, supervised by Prof. Dr. Ana Ledo and Prof. Dr. Rui Barbosa.

September 2022

FACULDADE DE CIÊNCIAS E TECNOLOGIA
UNIVERSIDADE D COIMBRA

CARBON NANOTUBE MODIFIED CARBON FIBER MICROELECTRODES FOR *IN VIVO* OXIMETRY IN AN ANIMAL MODEL OF TEMPORAL LOBE EPILEPSY

Submitted in Partial Fulfilment of the Requirements for the Master's Degree in Biomedical Engineering with speciality in Neuroscience

Author
João Miguel Fernandes Vieira

Supervisors
Ana Margarida da Cruz Ledo
Rui Manuel Silva Gomes Barbosa

Coimbra, September, 2022

This work was financed by the European Regional Development Fund (ERDF), through the COMPETE 2020 - Operational Programme for Competitiveness and Internationalisation and Portuguese national funds via FCT – Fundação para a Ciência e a Tecnologia, under project[s] POCI-01-0145-FEDER-028261 and UIDB/04539/2020, UIDP/04539/2020 and LA/P/0058/2020POCI-01-0145-FEDER-02826

This work was developed in collaboration with

We cannot solve our problems with the same
thinking we used when we created them.

Albert Einstein

Agradecimentos

Tendo chegado ao fim de mais uma etapa, gostaria de agradecer a todos os envolvidos.

Em primeiro lugar agradecer à Professora Doutora Ana Ledo pela oportunidade de poder pôr "mãos à obra" num laboratório e experienciar em primeira mão todos os resultados obtidos, obtendo experiência que outrora não tinha podido alcançar. Também por toda a orientação, esclarecimento de dúvidas e correção científica que foram essenciais para este trabalho. Agradeço também ao Professor Doutor Rui Barbosa e à Eliana Fernandes por todo o apoio, simpatia e disponibilidade prestados no laboratório.

Embora não envolvidos neste projeto, tiveram uma influência significativa para este se desenvolver quero também agradecer ao meu grupo de amigos: ao Pedro Miguel que teve um papel fundamental no meu percurso académico e social sendo a tua companhia essencial para conseguir terminar esta etapa, ao Luis, ao Daniel, ao Bernardo, ao João Pedro e ao Gonçalo por todos os momentos que irão sempre marcar estes anos e que guardarei comigo. Também agradecer à minha namorada Beatriz pela companhia e motivação no dia a dia para continuar mesmo quando não havia forças. A todos vocês muito obrigado.

Por fim, agradecer à minha família, especialmente pais, irmão e avós por todo o apoio nas diferentes etapas da minha vida e também à minha cadelinha e fiel companheira Lara. Não teria aqui chegado sem vós e também não teria conseguido concluir esta etapa sem vocês.

Abstract

Epilepsy is one of the most common and serious brain diseases which affects a large number of people, provoking diverse lifestyle consequences and limitations. It is many times hard to treat/control with medication and worldwide efforts have been undertaken to achieve disease control, which may allow patients to attain an independent lifestyle. The most common form of acquired epilepsy is temporal lobe epilepsy, since the temporal lobe is the most epileptogenic region of the human brain, also being one of the most common and intractable types of epilepsy that usually results from a trauma and only manifests its symptoms later in life.

The human brain is a highly complex and metabolically active organ, and as such an advanced and efficient vascular system is needed to meet the energetic demands in order to preserve the homeostatic balance of the brain. Even though this organ only makes up 2% of the overall body mass, it requires a high input of metabolic substrates to fulfil its needs, consuming about 20% of the total oxygen intake. Despite spending such a large amount of energy, the brain does not possess a way to store nutrients to use when needed. These necessities are suppressed by the blood supply and accurate and precise adjustment of cerebral blood flow as a function of activity level – neurovascular coupling. Compromised neurovascular coupling is associated with several disease states, including epilepsy.

Molecular oxygen plays a crucial role in maintaining a healthy brain function, and the mechanisms that control its usage and delivery are vital to preserve normal brain homeostasis. Besides its critical role in cellular respiration, where it is the terminal electron receptor of the mitochondrial respiratory chain, it originates reactive oxygen species that play an important signalling role in the regulation of the cerebral blood flow. Increased neuronal activity in a specific region of the brain is associated to an increment in cerebral blood flow as well as a change in oxygen consumption.

Considering this data, research on oximetry techniques, assessing brain pO_2 *in vivo* and in real time, is of considerable value to comprehend how oxygen affects various metabolic and disease states, as well as aiming to achieve treatment and therapy alternatives using the gathered data.

In this project we constructed carbon fibre microelectrodes (CFM) coated with multi-walled carbon nanotubes (MWCNT) in a Nafion® matrix for *in vivo* monitoring of pO_2 in the brain. These MWCNT-modified CFM were evaluated for their electroanalytical performance towards the electroreduction of oxygen and tested for their ability to adequately monitor dynamic changes in pO_2 *in vivo* in a model of 4-aminopyridine evoked seizures. Furthermore, we explored the capability of high-frequency amperometry to concurrently allow the measurement of pO_2 and electrophysiological data in the form of local field potential-related currents. The main goal was to study the changes in brain tissue pO_2 during paroxysmal events such as convulsive seizure in the hippocampus, a structure that is greatly impacted in Temporal Lobe Epilepsy.

The results support the notion that MWCNT coating has an electrocatalytic effect, lowering the overpotential needed for electrochemical reduction and monitoring of O_2 and increasing sensitivity as compared to bare CFM for working potentials between -0.5 and -0.8 V vs. Ag/AgCl. Regarding the *in vivo* studies, we found that 4-aminopyridine-evoked seizures produced biphasic changes in brain tissue pO_2 that were clearly correlated with increased neuronal firing observed as an increase in power at frequencies above 1 Hz.

This study confirms the benefits of MWCNT for oxygen measurements with CFM, the suitability of these electrodes for *in vivo* oxygen recording and also shows results that corroborate other studies with different chemoconvulsants that show the epileptic dip followed by a hyperoxygenation phase, showing the success and potential of this approach to acquire new data allowing better control of epileptic seizures.

Keywords: Epilepsy, Electrochemical sensors, Carbon-Fibre Microelectrodes, 4-aminopyridine, Electrochemistry, Carbon Nanotubes

Resumo

A epilepsia é uma doença cerebral comum que afeta um número elevado de pessoas, trazendo inúmeras alterações à qualidade de vida dos pacientes. Diversos estudos têm sido feitos de forma a encontrar formas de manter a doença controlada e providenciar às pessoas afetadas um estilo de vida mais independente, dado que esta ainda é uma doença incurável e é difícil controlar as convulsões. A região do cérebro mais epileptogénica é o lobo temporal e por isso, a epilepsia do lobo temporal é a forma mais comum de epilepsia, sendo também uma das mais difíceis de controlar.

Apesar de apenas representar apenas 2% do peso total do corpo, o cérebro humano requer uma quantidade elevada de substratos metabólicos para satisfazer as suas necessidades, consumindo sensivelmente 20% do oxigénio que entra no organismo. É assim dependente de um sistema vascular eficiente que fornece a energia necessária para manter o equilíbrio homeostático do cérebro. Apesar de necessitar de elevadas quantidades de energia, o cérebro carece de uma forma de reservar nutrientes para quando são necessárias reservas metabólicas de modo a satisfazer as necessidades energéticas. Para fazer frente a esta adversidade, o cérebro conta com os nutrientes presentes na corrente sanguínea que têm de ser distribuídos de forma precisa e exata, ajustando o fluxo cerebral sanguíneo consoante o nível de atividade cerebral- acoplamento neurovascular.

O oxigénio molecular é fundamental ao bom funcionamento do cérebro, e os mecanismos que controlam o seu uso e distribuição são vitais para preservar o equilíbrio homeostático do cérebro. Para além do seu papel fulcral na respiração celular, onde este é o recetor de eletrões final da cadeia respiratória mitocondrial, o oxigénio também é ainda necessário para a produção de espécies reativas de oxigénio que desempenham um papel importante de sinalização na regulação do fluxo sanguíneo cerebral. O incremento da atividade neuronal numa região especifica do cérebro está associado a um aumento do fluxo sanguíneo bem como a uma alteração do consumo de oxigénio.

Deste modo, a investigação focada no desenvolvimento de novas técnicas de oximetria, de maneira a aferir a pO_2 *in vivo* em tempo real, têm um potencial para permitir uma melhor compreensão de como o oxigénio afeta diversos estados metabólicos e de doença, assim como na procura de um tratamento e alternativas terapêuticas utilizando os dados adquiridos.

Neste projeto, construímos microeléctrodos de fibra de carbono (CFM) revestidos com nanotubos de carbono de múltiplas paredes (MWCNT) numa matriz de Nafion® para monitorização *in vivo* do pO_2 no cérebro. Estes microeléctrodos alterados foram avaliados quanto à sua performance eletroanalítica relativamente à eletroredução do oxigénio e testados no que toca à sua habilidade de medir corretamente alterações dinâmicas no pO_2 *in vivo* num modelo de convulsões provocadas por 4-aminopiridina. Para além disto, também foi explorada a capacidade da amperometria de alta frequência como forma de medir simultaneamente a pO_2 e informação eletrofisiológica na forma de correntes do potencial local de campo. O principal objetivo foi o de estudar as alterações no cérebro ao nível do pO_2 do tecido durante eventos com convulsões no hipocampo, uma estrutura altamente afetada pela epilepsia do lobo temporal.

Estes resultados vão de encontro com a noção de que os MWCNT possuem um efeito eletrocatalítico, diminuindo o potencial excessivo necessário para a detenção e monitorização eletroquímica do O_2, aumentando a sensibilidade, quando comparados a CFM sem revestimento, para potenciais de trabalho entre -0,5 e -0,8 V vs. Ag/AgCl. Em relação aos estudos *in vivo*, constatámos que as convulsões induzidas por 4-aminopiridina produzem alterações bifásicas na pO_2 do tecido cerebral que foram visivelmente relacionados com um aumento da atividade neuronal observada no aumento da potência em frequências acima dos 1 Hz.

Este estudo confirma os benefícios dos MCNT para efetuar medições de oxigénio *in vivo* com CFM, demonstrando ainda a aptidão destes elétrodos para efetuar medições de variações de oxigénio, assim como resultados que corroboram outros estudos realizados com outros convulsivantes químicos que demonstraram a queda inicial na concentração de oxigénio (“epileptic dip”) seguida de uma fase de hiperoxigenação, demonstrando o sucesso e potencial que esta técnica tem para adquirir novos dados com o objetivo de poder alcançar um melhor controlo das crises epiléticas.

Palavras-chave: Epilepsia, Sensores eletroquímicos, Microeléctrodos de fibra de carbono, 4-aminopiridina, Eletroquímica, Nanotubos de Carbono

Contents

List of Figures

List of tables

Abbreviations

4-AP	4-Aminopyridine
AED	Antiepileptic drugs
BOLD	Blood oxygenation level dependent
C	Concentration
CBF	Cerebral Blood Flow
CBV	Cerebral Blood Volume
CFM	Carbon fiber microelectrodes
CNT	Carbon Nanotubes
CV	Cyclic Voltammetry
D	Diffusion Coefficient
DG	Dentate Gyrus
DTI	Diffusion Tensor Imaging
EIS	Electrochemical Impedance Spectroscopy
EPR	Electron Paramagnetic resonance
ESA	Electroactive Surface Area
FCV	Fast Cyclic Voltammetry
FDG-PET	Fluorodeoxyglucose-Positron Emission Tomography
FFT	Fast Fourier Transform
fMRI	Functional magnetic resonance imaging
GABA	Gamma-Aminobutyric Acid
HbO	Oxyhaemoglobin
HbR	Deoxyhaemoglobin
HbT	Total Haemoglobin
IBE	International Bureau for Epilepsy
ILAE	International League Against Epilepsy
I_p	Anodic or Cathodic peak currents
IUPAC	International Union of Pure and Applied Chemistry
KA	Kainic Acid
LOD	Limit of Detection

MEA	Microelectrode Array
MRI	Magnetic Resonance imaging
MWCNT	Multi-Wall Carbon Nanotubes
n	Number of electrons involved in the redox reaction
NIRS	Near-infrared spectroscopy
NMR	Nuclear Magnetic Resonance
PBS	Phosphate-Buffered Saline
PET	Positron Emission Tomography
pO_2	Oxygen Partial Pressure
SD	Standard Deviation
SE	*Status Epilepticus*
SPECT	Single Photon Emission Computed Tomography
STFT	Short-Time Fourier Transform
TLE	Temporal Lobe Epilepsy
ν	Scan Rate

1. INTRODUCTION

Epilepsy is one of the most prevalent and serious brain diseases, affecting approximately 1% of people worldwide and having a variety of negative effects on lifestyle. Treating and controlling epilepsy is a huge obstacle that scientists and physicians have to overcome, so there are still a wide variety of studies being conducted in order to give people with epilepsy an improved lifestyle [1]. Temporal lobe epilepsy is the most prevalent form of epilepsy and also one of the hardest to control since the temporal lobe is a highly epileptogenic region in the human brain [2–4]. So, it is crucial to further understand this type of epilepsy and better comprehend biomarkers to achieve a way for epileptic people to stay independent.

Electrochemical measurements have been widely used to study different biomarkers that can help predict epileptic seizures such as glucose, lactate, oxygen (O_2), and others. Carbon fibre microelectrodes (CFM) have been used since they are cheap and easy to produce, being sensible and a reliable way to perform *in vivo* measurements [5]. However, the electroanalytical performance of CFM can be improved through surface modification, namely by exploring the electrocatalytic properties of nanomaterials such as carbon nanotubes [6,7].

The main goal of this project was to design and evaluate multi-wall carbon nanotube (MWCNT) modified CFM for *in vivo* electrochemical monitoring of O_2– oximetry - during chemoconvulsant induced epileptic seizures in the hippocampus. Furthermore, by performing high frequency amperometry coupled to signal processing, we aim to concurrently monitor O_2 and electrophysiological data in the form of local field potential-related currents, using a single probe [3,8]. Monitoring changes in tissue O_2 which result from neurometabolic and neurovascular responses during seizures can help us better understand the neuropathology of epilepsy. By further combining electrophysiological data, one may hope to further understand the intricate interplay between aberrant brain activity and the metabolic/cerebrovascular response in epilepsy.

1.1. Epilepsy

According to the International League Against Epilepsy (ILAE) and the international Bureau for Epilepsy (IBE), epilepsy is defined as a disorder of the brain characterized by an enduring predisposition to develop epileptic seizures and by the associated neurobiological, psychological, cognitive, and social repercussions [9]. The definition of epilepsy requires the occurrence of at least one epileptic seizure, described as a transient occurrence of signs and/or symptoms because of abnormal excessive or synchronous neuronal activity in the brain [9]. The process of developing epilepsy is defined as epileptogenesis [10].

Difficulties in harmonizing the diagnosis of epilepsy due to the lack of criteria prompted the ILAE task force to recently rectify the definition of epilepsy as a disease of the brain described by any of the following conditions [11]:

1. Occurrence of at least two unprovoked (or reflex) seizures more than 24 hours apart.
2. Occurrence of one unprovoked (or reflex) seizure, coupled with a probability of additional seizures equivalent to the general recurrence risk (at least 60%) following two unprovoked seizures, happening on the course of the 10 following years.
3. Detection of an epilepsy syndrome.

Additionally, epilepsy is considered treated for individuals with age-dependent epilepsy syndrome who have past the applicable age as well as in subjects who have remained seizure-free for the last 10 years, without seizure medicine for the last 5 years [11].

Epilepsy is one of the most prevalent serious brain diseases, with an incidence of approximately 1% worldwide, and it has significant social, psychological, and physical repercussions [1]. Risk factors vary with age and geographical location, and whereas epilepsy associated with head trauma, tumours and central nervous system infections can develop at any age, for people with more than 60 years, cerebrovascular disease is the most common risk factor [12].

Epilepsy is characterized by the sudden changes that occur in brain dynamics, leading to abnormal synchronization of extended brain networks, that are called seizures. These are generated in a process called ictogenesis and are distinguished by a transient impairment of sensation, thinking and motor control [1]. Due to their unpredictable nature, seizures impose restrictions in several domains such as lifestyle, career, relationship, besides other limitations the disease brings [1,13]. People with epilepsy experience decreased quality of life and require a change in their daily habits. Many become incapable of performing several tasks they did before, requiring assistance, and may experience progressive worsening of their condition [13]. Additionally, epilepsy is a stigmatizing condition, leading to discrimination and less employment opportunities [13].

The most common form of epilepsy in adults is temporal lobe epilepsy (TLE), since the temporal lobe is the most epileptogenic region of the human brain. TLE is particularly disabling, due to its unpredictability, linked to a poor response to antiepileptic drugs (AED) that frequently results in an indication for resection surgery [2–4]. This type of disease is a group of disorders that involves the dysregulation of hippocampal function caused by neuronal hyperexcitability and usually starts from epileptogenic events such as febrile seizures during early childhood, brain trauma, perinatal injury, congenital brain malformation, brain tumours infections on the central nervous system, or *status epilepticus* (SE) followed by a latent period in which the hippocampus develops atrophy, triggering spontaneous seizures [3,4,14].

1.1.1. Treatment

Several studies have aimed to better understand the neuromolecular mechanisms of epilepsy in the hope of developing effective treatments. The main path used to treat and suppress seizures without rectifying the underlying neuropathological process are AED and people with epilepsy frequently require a lifelong supply of AEDs [15].

The majority of antiepileptic drugs possess more than one mechanism of action [16]. The following classification of AED is based on their mechanisms:

1. Blockage of voltage-dependent sodium or calcium channels, preventing sustained repetitive firing in individual neurons. These AED show effectiveness against

generalized tonic-clonic and partial seizures. This group has several examples such as carbamazepine, oxcarbazepine, gabapentin, lamotrigine, topiramate, phenobarbital, phenytoin, valproate [16].

2. Enhancement of the inhibitory events mediated by GABA: benzodiazepines, gabapentin, phenobarbital, tiagabine, topiramate, vigabatrin, and valproate [16].

3. Blockage of T-type calcium channels, which is active against absence seizures. This group consists of a single drug, ethosuximide [16].

4. Reduction of events mediated by excitatory amino acids (like glutamate). There are currently three antiepileptics that meet these requirements: felbamate, phenobarbital, and topiramate [16].

In about 30-40% cases of patients with epilepsy, AED and other types of treatment are not capable of keeping seizures under control [17]. This type of epilepsy is called refractory epilepsy [17]. Refractory epilepsy can evolve over time, holding risks for structural brain and nervous system damage, comorbidities (osteoporosis, fractures), increased mortality (from suicide, accidents, sudden death, pneumonia, and other diseases), as well as psychological (depression, anxiety), educational, social (stigma, driving), and vocational repercussions [17]. In 2010 the ILAE published a definition of refractory epilepsy to help improve patient care and research, considering two levels disposed in hierarchy [17,18]. The first level considers the outcome in response to therapeutic interventions (seizure freedom, treatment, failure, or undetermined) while the second level classifies the drug responsiveness (Drug resistant, drug responsive or undefined) [17,18].

Since there is a therapeutic failure in about 30-40% of patients, intensive research for new antiepileptic drugs has been developed, bringing nine new and licenced treatments to patients that poorly responded to conventional therapy, including felbamate, gabapentin, lamotrigine, levetiracetam, oxcarbazepine, tiagabine, topiramate, vigabatrin, and zonisamide [16]. Other therapeutic options include surgery, brain stimulation and dietary intervention [15].

With the focus of achieving seizure control and improving the quality of life of patients with refractory epilepsy, physicians perform **surgical treatments of epilepsy** [19]. When it is possible to clearly identify a seizure-onset zone, resection of the involved

area of the brain might benefit patients [19]. These procedures can imply the resection of the medial structures of the temporal lobe, including hippocampus, amygdala, and entorhinal cortex [20]. Resections implemented on the cortex are guided by imaging results and intracranial electroencephalography [20].

Neurostimulation is an emerging treatment for neurological diseases that is currently in use [21]. It uses electrical pulses directly to or in the neighbourhood of the nervous tissue, regulating a pathological substrate to achieve a symptomatic or curative therapeutic effect [21]. Electrically stimulating the tenth cranial nerve or vagus nerve stimulation are forms of extracranial stimulation that were developed in the eighties and are available for routine treatments in epilepsy centres [21]. This technique is recommended in patients with refractory epilepsy that are not suited for surgery or who have had lack of results from treatment [21]. As for intracerebral neurostimulation, it requires access to the intracranial nervous system since electrodes are placed into intracerebral targets for deep brain stimulation or inserted over the cortical convexity for cortical stimulation [21]. This technique is still under development [21].

As for the **dietary intervention**, ketogenic diet (comprising very low carbohydrate combined with high fat content) and other related diets have been shown to have some efficacy in seizure reduction [17]. It was developed in 1921 with the objective of mimicking the anticonvulsant effects of fasting, which was previously known to suppress seizures and was widely used before the appearance of AED [22]. The ketogenic diet was used only used as a last resort until the 1990s, when it resurfaced as an important way to treat epilepsy in particular in children refractory seizures [22] According to studies, at least half of all patients treated with this diet show a 50% or greater reduction of seizure frequency [22]. Recent studies show that a ketogenic diet can sometimes be discontinued without losing the control of seizures, suggesting that it can be both anticonvulsant and antiepileptogenic [22].

1.2. Neurovascular and metabolic events associated with seizures

The human brain is one of the most sophisticated and metabolically active organs of the body and as such is supplied by a complex vascular system that is able to fulfil the energetic needs and supply energy substrates and nutrients, remove unwanted proteins and metabolites, facilitate neuroimmune trafficking, and maintain the homeostatic

balance of the brain [23]. Even though the brain only accounts for 2% of the total body mass, it is responsible for a high intake of metabolic substrates, consuming 20% of O_2 and 25% of glucose, and receiving approximately 15% of the cardiac output [24,25]. Furthermore, the brain lack a robust energy reservoir such as muscle [26]. Consequently, energy substrates including O_2, and glucose are supplied via a tightly regulated processes which allows accurate delivery to reach the brain area as a function of activity, at the right time and in the required amount [26,27]. The interruption of the blood supply to the brain for more than a few minutes leads to irreversible brain damage and also death [26]. Furthermore, even if the blood flow is only reduced and is not capable to match the energy demands of the tissue, more subtle brain modifications take place, possibly leading to chronic brain injury in more vulnerable areas that are often linked to cognitive impairment [26].

These precise energetic needs demand a precise supply that is obtained with the adjustment of local cerebral blood flow as a function of activity level, which is called neurovascular coupling [24]. Another key concept is neurometabolic coupling which is the activity-dependent balancing of glucose and O_2 utilization by neural cells [24]. As previously stated, glucose is the major energy source for the brain, although different studies have shown that the brain is also capable to use other alternatives such as lactate or ketone bodies during development or to fulfil any gap when glucose is limited [25].

During seizures, excessive neuronal activity imposes above normal energy demands, altering brain homeostasis significantly [24]. This is associated with profound neurometabolic and neurovascular changes [24,28]. The increasing neuronal activity originates transient hypoxia due to an augmented energetic need, which is closely followed by a robust increase in cerebral blood flow and hyperaemia, that is, a surplus of blood supply [24,27]. As the seizures advance, the hyperaemia declines while the metabolic rate remains high, draining the cerebral energy sources, which precipitates intracellular acidosis [24]. These seizures may also disrupt the blood-brain barrier and negatively impact cerebral auto-regulation mechanisms [24]. Considering this, monitoring O_2 and/or glucose is of interest, more so when combined with monitoring of brain tissue electrical activity [3,28,29].

Early studies using a wide range of animal models and employing imaging techniques such as autoradiography and later in humans using PET, SPECT, fMRI have shown evidence of a dramatic increase in cerebral blood flow and metabolism in the epileptic focus or epileptogenic zone, the area of the cerebral cortex where the epileptic seizures start, or the site with most ictal activity, while a seizure is initiated and propagates [30,31]. Adding to this, preictal hemodynamic events such as the increase in neuronal activity result in an increase in cerebral metabolic rate of O_2 and glucose, raising the cerebral blood flow [31–33]. Studies performed in animals and humans, using several imaging techniques have shown that the increase in cerebral blood flow to meet the increment in metabolism results in an increase in blood oxygenation, which can precede seizures from 20 minutes to a few seconds, exhibiting promise as a technique to recognize seizure onsets [30–32].

Studies performed in the bicuculline model (described in section 1.4.1) have shown a disturbance on neurovascular coupling [33]. By measuring alterations in oxy-, deoxy- and total haemoglobin (HbO, HbR and HbT), through near-infrared spectroscopy (NIRS) it was noticed that in the period that precedes the spike, an increment in HbO and HbT was perceptible, that may result from vasodilatation and a decrease in HbR, indicating a reduction in metabolic demand, meaning that there is a deactivation of the neuronal structure before an epileptic spike [34]. This period is swiftly followed by a swing back, decreasing HbO and Hbt and increasing HbR, a stage known as the "initial dip", in which a drop in local tissue O_2 before the outbreak of the spike is observed [34]. Succeeding the spike, there is an inverse response in order to restore homoeostasis [33].

1.2.1. Neurometabolic markers in epilepsy

Normal brain function requires continuous energetic supply, and as such, neurometabolic dysfunction is a key pathophysiologic aspect of the epileptic brain [34].

In the aftermath of an epileptogenic insult, several factors, including environment, treatment attempts and others, can alter the outcome of the disease [35]. An effort has been made to identify and measure reliable biomarkers and surrogate disease markers of epileptogenesis, which hold the potential to aid clinicians in identifying patients at high risk of developing epilepsy following a brain insult (febrile seizures, status epilepticus,

head trauma, or brain inflammation) [35]. *In vitro* and *in vivo* models have been used for several decades in order to study the molecular and cellular mechanisms behind the occurrence of spontaneous recurrent seizures [35]. However, the pathogenic mechanisms that generate the epileptic conditions, particularly after precipitating events are still not well understood [35]. In this context, monitoring neurometabolic markers including O_2, glucose, and lactate, hold great promise [35].

Molecular O_2 plays a key role in maintaining a healthy brain function and the mechanisms that monitor the delivery and usage of O_2 are essential to preserve normal brain homeostasis, physiology, and energy metabolism [36]. Pathophysiological issues can be an outcome of any shortcoming in cerebral tissue partial pressure of O_2 (pO_2) levels, leading to the increased production of reactive O_2 species, inducing oxidative stress [36]. The present knowledge of the connection between neuronal activity and O_2 metabolism still has many gaps and there are possibly several mechanisms and regulatory pathways yet to be unveiled [37]. Hypoxia is one of the key regulatory mechanisms on the brain, being neurons and the neuronal functions highly sensitive to hypoxia and the interruption of O_2 supply can induce severe damage to the brain within a short time and also secondary effects affecting protein function and gene expression [37]. As we can observe by the data gathered, it is now understood that increasing the neuronal activity in a specific region of the brain is linked to an increase in blood flow, associated to respective O_2 changes [38].

Acknowledging this, studies in oximetry methods, evaluating cerebral pO_2 *in vivo* and in real time are of great relevance to understand how O_2 influences various metabolic and disease states and to try to achieve treatment and therapy options with the data acquired [36].

Early studies performed in 1936 measuring O_2 saturation in arterial blood found a slight decrease in patients with epilepsy, although this hypoxemia was not found to be exclusive to epilepsy [39]. Despite the lack of mechanistic explanation for their observation, this study highlights the early interest in understanding how changes in O_2 supply might be associated with seizures and epilepsy.

More recent clinical and pre-clinical studies have focused on local changes in brain tissue O_2 based on the concept of neurovascular coupling [40,41]. By monitoring

pO_2, studies have revealed that epileptiform activity produces a biphasic response in tissue *p*O_2 during ictal events [3]. The initial phase is characterized by a decrease in *p*O_2 as a result of increased cerebral metabolic rate for O_2, which has been classified has the epileptic dip and has been shown in studies to have a predictive value, as it may precede the occurrence of an epileptic seizure [3,42]. The following phase consists of a persistent increase in tissue *p*O_2 has a result of a diffuse increase in cerebral blood flow (called hyperaemia) and metabolic changes [3].

Besides O_2 other relevant neurometabolic markers in the context of epilepsy and seizures activities include glucose and lactate. Studies using FDG-PET imaging performed in a rat model of epilepsy induced by pilocarpine (described in section 1.4.1.2) showed a considerable increase in glucose metabolism in the hippocampus and entorhinal cortex during *status epilepticus* and hypometabolism in the limbic structure and thalamus during the first stages of epileptogenesis [43,44]. One other study performed using both kainic acid and pilocarpine models of epilepsy demonstrated a sharp spike in brain glucose metabolism after acute seizures, showing increased metabolic activity, especially in the hippocampus [43,45].

Besides these 2 canonical energy substrates, interest has increased regarding lactate. Despite being classified during decades as a metabolic waste product of glucose metabolism in anaerobic tissues, several studies have shown that neurons can use lactate as a metabolic substrate in aerobic conditions [46]. Lactate is a main source of fuel for the brain metabolism and provided locally from aerobic glycolysis or from peripheral circulation [47]. It is produced around the brain, especially in cells with few mitochondria, like the astrocytes [47]. Studies using kainate in mice have shown that lactate concentrations were significantly higher in the kainate-injected hippocampus than the control ones that were injected with saline [48]. With these results we can see that lactate levels are increased in the hippocampus when using a chemoconvulsant, making it a good biomarker to study epilepsy [48,49].

In the present work we will focus on monitoring *p*O_2 in brain tissue *in vivo*, coupled to monitoring the electrical activity of neuronal cells.

1.3. Monitoring brain tissue *p*O_2

Several disorders result in important changes in brain tissue *p*O_2 levels, including traumatic brain injury, stroke, and seizures, most of which are accompanied by hypoxia [49]. Epilepsy, in particular, places an above average demand on the autoregulatory mechanisms of the brain since the normal neuronal metabolism of O_2 tremendously increases after both interictal and ictal events [49]. Additionally, high levels of O_2 in tissues can lead to O_2 toxicity and neuropsychiatric disorders [49]. For this reason, monitoring O_2 levels is of vital significance [49].

There are presently several approaches towards measurement of *p*O_2 in brain tissue. Quantitative measurements of *p*O_2 *in vivo* have been collected using both invasive and non-invasive methods such as (i) fiber-optic fluorescence, (ii) near-infrared spectroscopy (iii), positron emission tomography (PET), (iv) nuclear magnetic resonance (NMR), and (v) electron para-magnetic resonance (EPR) [50].

Fast absolute measurements of *p*O_2 can be achieved using O_2-dependent quenching phosphorescence, an optical method with excellent specificity, high sensitivity, and simple implementation, used for O_2 sensing in biological systems [51]. With the development of phosphorescent probes that are water-soluble and nontoxic, the O_2 concentrations can be investigated in greater detail [51].

Near-infrared spectroscopy (NIRS) is particularly well suited for capturing haemodynamic signals in both clinical and pre-clinical studies by taking advantage of the absorbing properties of living tissues in the near-infrared range [33]. Nuclear magnetic resonance (NMR)-based oximetry has also been utilized effectively *in vivo* to quantitatively examine *p*O_2, having potential for usage in clinical settings [52].

Tissue oxygenation in can also be determined *in vivo* using Electron Paramagnetic resonance (EPR), a technique that can detect and characterize molecules that have unpaired electrons, an allows assessment of different biological parameters including tissue *p*O_2 *in vivo* in real time [52]. Minimally invasive procedures are required to insert the paramagnetic substance in the target region and the succeeding measurements are non-invasive [53]. This technique presents high sensitivity, good accuracy, reproducibility, and allows repetitive measurements, responding to variations usually in

less than 1 minute [36]. The method is suitable for use on awake, restrained animals as well as on anesthetized animals [53].

In recent times, studies have been developed in order to investigate the changes in brain tissue pO_2 by inducing stimulus, increasing neuronal activity, mainly because of modern non-invasive brain imaging techniques like positron emission tomography (PET) and functional magnetic resonance imaging (fMRI) [54]. To gather intel, these techniques rely on neurometabolic, and neurovascular coupling and the signals associated, in search for a superior knowledge on brain tissue oxygenation [54].

To fulfil the metabolic needs of the brain, O_2 is transported by the haemoglobin molecule [54]. The magnetic properties of endogenous haemoglobin are used in BOLD fMRI to gather the changes in activity in the function of the brain, lacking the need for exogenous tracers that are used in PET, being this technique based on the differing magnetic properties of oxyhaemoglobin and deoxyhaemoglobin, allowing to know or estimate the values of the cerebral blood flow, cerebral blood volume and the cerebral metabolic rate of O_2 consumption [54].

In vivo imaging techniques are a powerful non-invasive tool in neurochemical research due to their nature that allows three-dimensional visualization of neural activity across broad spatial scales, from the molecular level to the intact brain [55]. Magnetic resonance image (MRI) is one of the most versatile clinical and research tools, allowing high-resolution images of the brain over long periods of time to be obtained [43]. It has been used to detect structural, functional, and metabolic alterations in the intact brain [43]. Diffusion Tensor Imaging (DTI) is one imaging tool that provides a high tissue contrast based on microstructural characteristics of water diffusion [35].

Polarographic microelectrodes were used to produce the majority of the existing data on brain tissue pO_2 [56]. Under the influence of a negative polarizing voltage, O_2 is reduced at the surface of a noble metal in polarography [56]. The polarographic electrode typically comprises of a nearby or built-in reference electrode and a membrane-covered cathode where O_2 is reduced [56].

In vivo electrochemical sensing has been contributing with a new understanding in analytical neurochemistry, due to its excellent spatial and temporal resolution. Electroactive species such as O_2 can undergo redox reactions at the surface of the implanted microelectrodes, producing current or potential signals that reveal quantitative

and qualitative characteristics of the analyte. Some important examples of techniques that are used to study these alterations are Fast-scan cyclic voltammetry, amperometry and galvanic redox potentiometry [57]. Amperometric measures coupled to small or ultra-small probes offer both high temporal and spatial resolutions [58].

1.3.1. Electrochemical sensors

Using implantable microelectrodes to perform *in vivo* electrochemical sensing is a propelling strength in analytical neurochemistry [8]. Since the neurochemical networks have a high complexity, these measures impose demanding standards on electrochemical sensors, including selectivity, sensitivity, high spatiotemporal resolution and minimized disturbance on brain function [8]. In aqueous solution at neutral pH, the electrochemical detection of O_2 is based on its full 4-electron reduction to water.

$$O_2 + 4e^- + 4H^+ \rightarrow 2H_2O \quad (E^o = 1.23 \text{ V vs. RHE})$$

This reaction can occur at the surface if an electrode given the suitable working potential is applied [50]. The first O_2 electrode was designed by Leland Clark in 1950 and received it´s invertors name [60]. The Clark electrode consists of a platinum cathode were O_2 is reduced and an Ag anode, separated from the measurement media by a gas-permeable membrane [59]. Although platinum is undoubtably an optimal electrode surface for the O_2 reduction reaction [60,61], its high price can render the production and routine use of disposable microelectrodes difficult. The O_2 reduction reaction is less favourable on carbon surfaces, however, the electroanalytical properties of carbon such as glassy carbon or carbon fibres can be improved through the use of nanomaterials such as carbon single and multiwall nanotubes [62].

Sensors are commonly produced of carbon-based materials due to their great electrical conductivity, adaptable nanostructures, and strong biocompatibility [63]. Carbon Nanotubes (CNT) are allotropes of carbon that present great benefits due to their low cost, extensible synthesis, and chemical stability and can be either single- or multi-walled (SWCNT and MWCNT, respectively) [63]. Since their first reports in 1991 (single-walled) and 1993 (multi-walled), several experiments have been conducted in

order to better understand and take advantage of the characteristics of these materials, developing several methods to synthesize them [63,64]. Carbon nanotubes present several exceptional physical proprieties such as tensile strength and electrical and thermal conductivity, whilst possessing low density and resistivity, surpassing cutting-edge bulk materials [64,65]. Nevertheless, after several decades of study these still lack the capability to replace several materials since science has yet been unable to transfer the superior nanoscale proprieties of CNT into macroscopic materials, forcing researchers to develop techniques to extrapolate these advantages to macroscopic materials such as carbon fibres [64].

Carbon nanotubes have been used to fabricate electrochemical sensors and biosensors due to their unique proprieties stated above, offering these sensors a handful of advantages such as high surface-to-volume ratio, promoting electron transferring reactions, increasing sensitivity, and reducing surface fouling, enhancing electrocatalytic activity [6,66]. An obstacle presented while using CFM is that they are unable to achieve certain levels of surface area, meaning very weak electronic signals that require very sensitive instrumental detection [66]. In order to face this adversity, CNT are used and deposited on the surface of the carbon fibre to obtain an improved surface area, whilst not changing the size of the electrode [66]. The deposition of CNT was previously attempted on a single carbon microelectrode before through dipping the CFM into a CNT suspension, aided by dispersing agents [66,67]. Suspensions of CNT in Nafion® have also been used to deposit these nanotubes on the electrode by dip coating and by electrochemical deposition [66]. Summing up, CNTs bring to the table several favourable proprieties that are required for high performance biosensors, such as CFMs which are used in this study.

1.3.2. Concurrent measurement of electrochemical and electrophysiologial activity in brain tissue

Neurons communicate using electrical and chemical signals and, in the last few decades, neurophysiology has made significant advances by introducing a variety of methods in extracellular electrophysiology and voltammetric neurochemistry [8].

To better understand how endogenous neurochemicals may modulate brain activity, simultaneous acquisition of *in vivo* electrophysiological and neurochemical information is fundamental [8]. Several strategies have been used in order to simultaneously record electrophysiological and electrochemical signals in brain tissue, including the use of 2 separate sensors for each modality placed in close proximity or a single sensor alternating between recording modes [29]. The seminal work of Zhang *et al*. showed that using a seamless electrochemical method – amperometry – one can extract both electrochemical and local field potential information. Indeed, amperometric signals obtained with a high frequency of acquisition can be separated in a low frequency component (<1Hz) which reflects the electrochemical signal resulting from electron transfer phenomena that occur at the electrode surface (redox reactions) while the high frequency component (>1Hz) rather resemble local field potential in several aspects, such as: coherent spectral fluctuations; clear characterization of different brain states and exhibits identical hippocampal theta depth profile [8]. These studies revealed that both local field potential (electrophysiological information) and neurochemical information can be obtained at the same time from electrochemical sensors alone. This work was initially performed using a choline-oxidase based biosensor using a platinum microelectrode array (MEA) as support but has since been replicated and confirmed using a similar Pt-MEA configured for dual glucose and lactate biosensor [28] and bare Pt-MEA for O_2 measurements [3], as well as Pt/Ir wire-based choline biosensor [68]. To date, and to the best of our knowledge, this has not been attempted using CFM or carbon-nanotube-modified CFM.

1.4. Pre-clinical Epilepsy Models

To study epilepsy a variety of models have been established, since the full comprehension of the mechanisms behind epileptogenesis and seizure generation in the temporal lobe epilepsy and other forms of epilepsy cannot be achieved solely from clinical studies with humans [69]. A great portion of the knowledge that has helped understand epileptic disorders comes from appropriate animal models [70]. There are several animal models that are used to provide a greater comprehension, which are summarized in the following sections.

1.4.1. Chemoconvulsants

Certain models use a systemic administration of chemoconvulsants to induce an initial precipitating injury (*status epilepticus)*, leading to the appearance of recurrent seizures originating from limbic structures [71]. In order to generate rodents with spontaneous recurrent seizures, chemoconvulsants such as 4-aminopyridine, pilocarpine, and kainic acid have been used [71,72]. There are several types of chemoconvulsants models in use.

1.4.1.1. 4-Aminopyridine model

4-Aminopyridine (4-AP) was developed in the 1960's as an avicide (Avitrol®) [73]. 4-AP is a known vasoconstrictor and selectively blocks voltage-gated potassium channels, increases calcium influx, prolongs the action potential and, as a result, enhances interneuronal and neuromuscular synaptic transmission [73]. It can also enhance the release of acetylcholine and studies have reported that this leads to dopamine transmission in rat striatum [73]. 4-AP has been extensively used as an *in vivo* model of epilepsy for the last three decades since it intensifies neuronal activity and provides scientists with the ability to mimic the encephalographic activity recorded in patients with partial epilepsy [34,72–75].

This model presents advantages to the current project since it has been used for similar studies as described in [42], in which ictal discharges had been induced by a local injection of 4-AP with the results of the experiments not being affected by its proprieties [42]. Also, this model has produced results for the detection of antiepileptic proprieties across substances with different mechanisms of action [76].

1.4.1.2. Pilocarpine Model

Muscarinic receptors influence the brain by taking part in processes like memory, learning, movement control, temperature control and in the modulation of signalling by other neurotransmitters [77]. Pilocarpine is a muscarinic agonist that is frequently used to induce seizures in animal rodent models for the study of epilepsy, since it produces a phenotype that resembles to human TLE [77]. It is highly isomorphic since it reproduces a large variety of characteristics present in the TLE. Pilocarpine administration induces

an elevation in glutamate levels in the hippocampus, followed by the appearance of seizures. The ensuing imbalance between excitatory and inhibitory transmission generates *status epilepticus* (SE) characterized by tonic-clonic generalized seizures. After several hours, the animal enters a seizure-free latent period followed by spontaneous recurrent seizures that characterize the chronic epileptic condition [2]. The main advantage of the pilocarpine model is its reliability, since it is possible to observe rats injected with pilocarpine developing spontaneous seizures, independent of the duration of the SE, requiring fewer injections [71].

1.4.1.3. Kainic Acid\Kainate model

This model presents high reproducibility in a wide variety of species using systemic, intrahippocampal or intra-amygdaloid administrations [78]. Kainic acid (KA) is a cyclic analog of L-glutamate and an agonist of ionotropic kainic acid receptors [78]. KA induces a prolonged excitatory response, reproducing the phenomenon observed in TLE since KA-induced seizures produce patterns of activity-induced neuronal cell loss and astrogliosis that closely resemble the neuropathology ("hippocampal sclerosis" or "Ammon's horn sclerosis") characteristic of TLE in humans [78]. The way that kainate affects inhibition is still unclear [79]. Nevertheless, some studies show that there is a direct depression of GABA release, mediated by a metabotropic action of kainate receptor activation [79]. Another possibility, kainate can also act indirectly by depolarizing interneurons and triggering spontaneous GABA release [79]. It is presumed that kainate depolarizes interneurons through the same dendritic receptors that contribute to kainate receptor mediated synaptic currents [79].

This model allows the study of ictogenesis and epileptogenesis and provides a better knowledge about TLE and has also contributed to the development of more efficient therapeutic drugs, remaining a widely used animal model on the study of TLE [78].

1.4.1.4. Other Examples

1.4.1.4.1. GABA inhibitors

There are several other chemoconvulsants that act as gamma-aminobutyric acid (GABA) inhibitors on the brain of several animal models such as bicuculline that has been utilized for studies in the mammalian central nervous system [80]; Pentylenetetrazol that acts as a GABA-A receptor agonist, suppressing the function of inhibitory synapses, increasing neuronal activity [81]; Picrotoxin that also acts as a GABA-A channel blocker, experimented in animal models of guinea pigs and others, being employed to analyse the mechanisms of convulsant activity by blocking calcium channels on epileptic activity [82].

1.4.1.4.2. Penicillin

Previous studies also used penicillin in feline models, by intramuscular injection of a large dose, showing a large resemblance to human generalized epilepsy characterized by absence attacks [83]. These previous conclusions suggested that postsynaptic inhibition might play an important role in the mechanism of some forms of generalized epileptic discharge [84].

1.4.2. Electrical Stimulation

This type of animal model consists in studying seizures induced by electrical stimulation which provides great advantage since it allows to reproduce epileptogenic features in the intact brain with low mortality and high reproducibility [71]. The most studied model in electrical stimulation is kindling [71], a seizure-induced plasticity phenomenon that manifests by electrical stimulation in specific brain regions and causes a progressive intensification of seizure susceptibility [69]. This model results in the emergence of spontaneous seizures and causes a permanent epileptic state [69].

Kindling can target a specific region of the brain and the parameters are easily manipulated by the experimenter [78]. However, this method is time-consuming since each animal needs to undergo repetitive electrical stimulation sessions [78].

1.5. Objective

Taking into consideration the state of the art that was presented, the main objective of the present work is the design and evaluation of the analytical properties of MWCNT-modified CFM for *in vivo* monitoring of pO_2 in the brain of anesthetized rodents upon 4-AP evoked seizures. The specific objectives include:

1) Construction and surface modification of CFM coated with MWCNT in a Nafion matrix;
2) Evaluation of the electrocatalytic effect of MWCNT on the O_2 reduction reaction;
3) Validation of MWCNT-CFM as an analytical tool for *in vivo* oximetry;
4) Concurrent monitoring of pO2 and local field potential related currents in a 4-AP model of seizures.

2. MATERIALS AND METHODS

2.1. Reagents and solutions

All chemicals were of analytical grade and supplied by Merck, unless otherwise stated. Argon and O_2 were provided by Air Liquide, Portugal. The carbon fibre microelectrodes were tested in 0.05 M phosphate buffer saline (PBS) at pH 7.4 with the following composition: 100mM NaCl, 10mM NaH_2PO_4 and 40mM Na_2HPO_4, prepared with ultra-pure Milli-Q deionized water (≥18 MΩ cm) (Millipore Company, Bedford, MA, USA). For the electrochemical active surface area measures, $Ru^{III}(NH_3)_6$ 5mM in KCl 0,5M was used. For modification of CFM surface with CNT, multiwall CNT (MWCNT, Nano-lab, USA) were suspended in a 0.5% Nafion® (prepared by dilution of the 5% Nafion® solution in isopropanol) to a final concentration of 10 mg/mL. For the *in vivo* tests, 4-AP was obtained from Tocris Bioscience. Saturated O_2 solution for calibration of CFM was prepared by bubbling pure O_2 gas into PBS for at least 20 min. At room temperature, the final concentration of O_2 under these conditions is 1.3 mM [85].

2.2. Carbon Fibre Microelectrodes

2.2.1. Fabrication and general evaluation

The CFM used were produced as described previously [86]. Briefly, a single carbon fibre (33 μm of diameter, Textron Lowell, MA, USA) was inserted into a borosilicate glass capillary (1,6mm i.d x 2mm o.d.) (Harvard Apparatus, Holliston, MA, USA) filled with acetone. Acetone is used to clear some impurities that the capillary may have and to minimize the electrostatic attraction between the capillary and the fibre. After the evaporation of the acetone, the capillary was pulled in a vertical puller (Harvard Apparatus Ltd.).

The protruding carbon fibre was cut to a length between 150 and 250 μm, using tweezers and an optical microscope (Olympus, U.S.A). Conductive silver paint (RS, UK) was inserted through the open end of the capillary to the shank, followed by a previously

laminated cooper wire that was sealed to the capillary with cyanoacrylate adhesive [87]. A schematic representation of the CFM is presented in Figure 1.

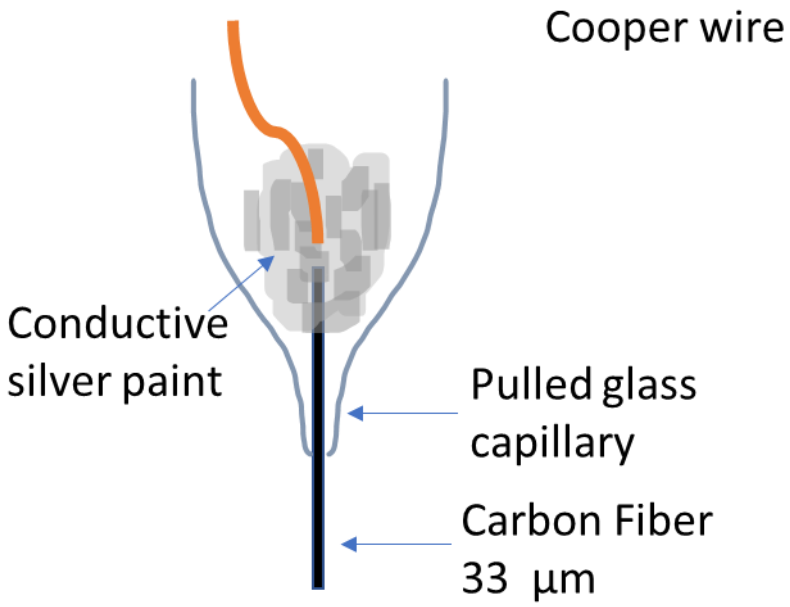

Figure 1. Schematic representation of a carbon fibre microelectrode.

Each CFM was tested for general recording properties by fast cyclic voltammetry (FCV) in PBS 0.05M, pH 7.4, between -0.4 and 1.6 V vs. Ag/AgCl, at a scan rate of 400 V s^{-1}. As shown in the cyclic voltammogram in Figure 2, CFM with good recording properties displayed sharp transition at reversion potential.

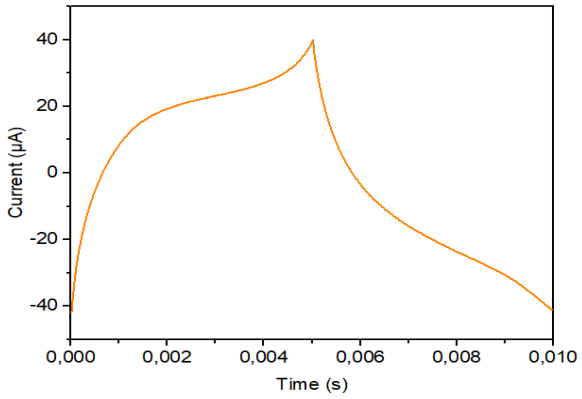

Figure 2. Representative voltammogram of a CFM with good recording properties.

2.2.2. Carbon Fibre Microelectrode Surface Modification

Carbon fibre microelectrodes were modified by deposition of MWCNT. To this purpose, each CFM was dipped in a 10 mg ml^{-1} suspension of MWCNT prepared in a 0,5% Nafion® solution. The suspension was placed in an ultrasound bath for 30 minutes to guarantee the dispersion of the MWCNT. The CFM tip was dipped in the suspension and stirred slowly for about 30 seconds and then dried at 170ºC for 5 minutes [6].

2.2.3. Electrochemical Methods

The electroanalytical properties of the MWCNT-modified CMF were evaluated through a series of electrochemical tests, which are described in detail bellow. For all methods, a 2-electrode electrochemical cell was used, comprised of a CFM as a working electrode and an Ag/AgCl (3M NaCl) reference electrode (RE-5B, BAS Inc., IN, USA).

2.2.3.1. Electroactive Surface Area

In order to determine the change in electroactive surface area induced by modification of the CFM surface with MWCNT, we explored the reversible redox reaction of hexaminerutheniu m (III). Cyclic voltammograms were obtained in a 5 mM solution of $Ru^{III}(NH_3)_6$ in KCl 0.1M. The potential was varied between -0,6V and 0,4V, at a scan rate varying between 25 and 200 mV s^{-1}. For each scan rate, anodic and cathodic peak currents (I_{pa} and I_{pc}, respectively) were measured and used to determine the electroactive surface area of the CFM from the Randles-Sevcik equation (Eq. 1)

$$I_p = 268600\, n^{2/3} A\sqrt{D} C\sqrt{\nu} \qquad (1)$$

where I_p represents the anodic or cathodic peak current, n is the number of electrons involved in the redox reaction (in this case n=1), A is the electroactive surface area, D is the diffusion coefficient ($9{,}10 \times 10^{-6}$ cm^2 s^{-1}, [88]), C is the concentration and ν is the scan rate. This was performed in bare and MWCNT-modified CFM.

2.2.3.2. Cyclic Voltammetry

In order to determine whether MWCNT modification of the CFM induced a change in the O_2 reduction potential, cyclic voltammetry (CV) was performed. This method consists of cycling of the potential applied at the working electrode immersed in an unstirred solution while measuring the resulting current [46]. In the present study cyclic voltammograms were obtained in PBS with a scan rate of 0,05 V s^{-1}, between -1,0 and 1,0V vs. Ag/AgCl. This was performed in bare and MWCNT-modified CFM.

2.2.3.3. Impedance Spectroscopy

Electrochemical impedance spectroscopy (EIS) is a powerful frequency domain technique that can provide us a powerful insight in physical phenomena occurring at the electrochemical interface [91]. It has been reported that electrode impedance has a direct impact on electrochemical performance for molecular sensing [91]. There are models of equivalent circuits that can assign individual circuit elements to physical proprieties of the electrochemical system [89].

In our impedance studies, our main goal will be to obtain an α_1 value, studying the EIS, being this value attributed to roughness, giving us information about how the surface of the electrode has been altered from the coating performed on the electrode. Studying this value will give us the information whether the coating changed the surface the electrode or if it doesn't bring any difference.

To accomplish this goal, we proceeded to the impedance studies before and after coating. These recordings were made in N_2-flushed PBS lite (pH=7.4) at room temperature, applying a sinusoidal wave of amplitude 0.01V between 100 kHz and 0.1 Hz. Relevant parameters were determined by fitting the experimental data to an equivalent circuit.

2.2.3.4. Sensitivity

Sensitivity is defined by IUPAC as the slope of the calibration curve, and it gives us the information of the sensor's capacity to measure in small analyte concentration alteration [90].

CFM were calibrated for O_2 using constant potential amperometry. Calibrations were performed in 0.05 M PBS pH 7.4 at room temperature (20ºC). O_2 was removed by bubbling N_2 gas and then maintaining the needle above the surface in order to decrease the O_2 back-diffusion to the calibration medium. Calibrations were performed in a range of -1.0V to -0.2V vs. Ag/AgCl by adding 200 µL aliquots of a 1.0 mM O_2 saturated solution to 20 mL Argon-purged PBS, at room temperature (20 ºC). (Figure 3)

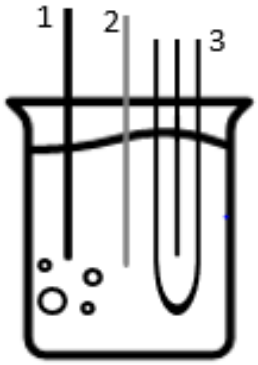

Figure 3. Scheme of the calibration experiment (1-Needle bubbling the N_2 gas; 2-Electrode (CFM); 3-Reference electrode)

To check the effect the coating brought to our electrodes, we then proceeded with the same experiments as stated before. Both bare and modified CFMs were calibrated for O_2 using constant potential amperometry using a FAST16 mKII in a 2-electrode configuration, using an Ag/AgCl/NaCl (3M) reference electrode.

2.2.3.5. Instrumentation

Electrochemical experiments involving cyclic voltammetry and impedance spectroscopy were performed using a Multi PalmSens4 Potentiostat (PalmSens, The Netherlands) controlled by MultiTrace v.5.8 software (PalmSens, The Netherlands).

Calibrations and *in vivo* recording of pO_2 were performed using a FAST16mkII potentiostat system (Quanteon, LLC., USA).

2.3. Animal Procedures

The suitability of modified CFM to monitor changes in brain tissue pO_2 was evaluated *in vivo* in the brain of an anesthetized rat with isoflurane. Using stereotaxic surgical procedures, the CFM-MWCNT/NAF mounted in an array with a micropipette was placed in the motor cortex of the rat (AP=-0,2; ML=1,0; DV=1,5 mm). Changes in pO_2 were elicited by local puff application of KCl (70 mM) at a distance of 200 µm from the CFM-MWCNT/NAF recording tip.

If this experiment was successful, studies will proceed to verify pO_2 variations on the hippocampus, after the injection of 4-aminopyridine.

For *in vivo* experiments, we used the CFM-MWCNT/NAF as the working electrode, and pseudo-reference produced by anodization of the exposed tip of a Teflon-coated Ag wire (200 µm o.d., Science Products, Germany) in 1 M HCl saturated with NaCl, which, when in contact with cerebrospinal fluid in the brain containing chloride ions, develops a Ag/AgCl half-cell.

The experiments in this project were all performed in accordance with the European Community Council Directive for the Care and Use of Laboratory Animals (2010/63/EU) and were approved by the local institutional animal care committee. For this study, 3 adults male Wistar rats (8-12 weeks, weight around 250 and 350g) were used. Previous to the experiments, these animals were handled and cared at the animal house facilities of the Centre for Neurosciences and Cell Biology (Coimbra), being maintained in a 12:12 light: dark cycle, having food and water available ad libitum [6,91].

Afterwards, the rats were anesthetized with urethane (1.25-1.50 g/kg, i.p) and posteriorly placed in a stereotaxic frame (Stoelting Co., USA), being the body temperature maintained at 37ºC using a delta phase isothermal pad (BrainTree Scientific, MA, USA). A craniotomy was performed aiming to expose the area of interest of the brain and, after removing the dura mater, the CFM/micropipette array was lowered into the rat hippocampus, using previously determined coordinates with the aid of a hydraulic micromanipulator (Narishige International Limited, UK) [6,91]. The specific coordinates

used in each experiment are indicated in each experiment result display on the next chapter.

For each experiment, a new reference of Ag/AgCl reference electrode (200 μm diameter) was prepared using a silver wire (GoodFellow, UK) in a HCl (1 M) solution saturated with NaCl and by applying a voltage of 1.5 V for 10 min [6,91]. To place this reference, a small hole was drilled into the skull of the rat far from the recording areas, being this reference inserted afterwards through the skull opening into the brain [6,91].

After the stabilization of the baseline current, KCl and 4-AP were locally pressure ejected into the brain from the glass micropipette using a Picospritzer III (Parker Hannifin Corp., General Value, Fairfield, NJ, USA), adjacent to the CFM sites. During these experiments, the skull and exposed brain surface of the animal are regularly sprinkled with saline to avoid the drying of the brain surface [6,91]. After the experiment was concluded, the animal was euthanized

2.4. Data Analysis

The data treatment and the graphics obtained and shown were obtained using Graphpad Prism 8 (GraphPad Software, U.S.A), Origin 2016 (OriginLab Corporation, U.S.A), PSTrace 5 (PalmSens BV,nHouten, The Netherlands) and EIS spectrum analyser [92]. To analyse the data obtained, we used FAST Analysis version 6.0.

3. RESULTS

In this chapter are gathered the results that were acquired from the studies performed on the CFMs, the effect of the coating and the *in vivo* experiments.

3.1. Electroactive Surface Area

In order to determine the electroactive surface area of bare CFM and MWCNT-modified CFM (CFM-MWCNT/NAF), we obtained cyclic voltammograms in a solution of $Ru^{III}(NH_3)_6$ at different scan rates. As can be observed in Fig. 4 there are a well-defined symmetrical oxidation and reduction peaks, starting at 25 $mV\ s^{-1}$

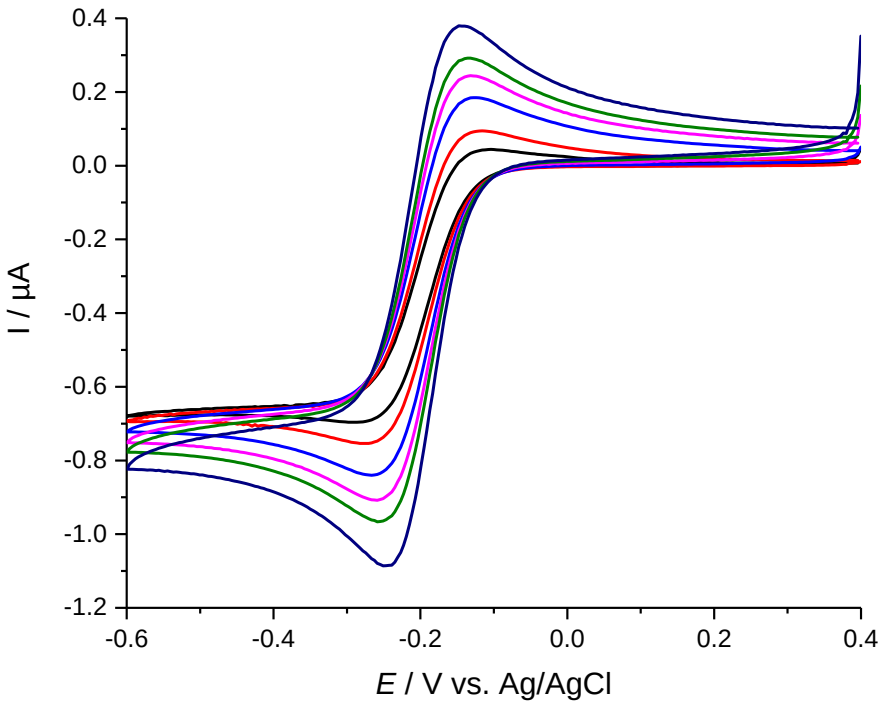

Figure 4. Reversible redox reaction of $Ru^{III}(NH_3)_6$ in 0.1 M KCl at increasing scan rates (from 25 mV s^{-1} in black to 200 mV s^{-1} in purple) for a CFM-MWCNT/Naf.

From the voltamograms obtained at 50 V s^{-1}, we determined the average ratio between anodic and cathodic current peaks (I_{pa}/I_{pc}) as well as the average half-width potential ($E_{1/2}$) for the reversible reaction.

Table I – Average values of I_{pa}/I_{pc} and $E_{1/2}$ calculated for the CFM and CFM-MWCNT/NAF from cyclic voltammograms obtained at 50 mV s^{-1} in 5 mM $Ru^{III}(NH_3)_6$ in 0.1M KCl.

DESIGN (N=6)	I_{PA}/I_{PC}	$E_{1/2}$ / V
CFM	-0.92 ± 0.01	-0.203 ± 0.002
CFM-MWCNT/NAF	-0.93 ± 0.03	-0.207 ± 0.002

As we can see, for both designs the ratio between peak currents is close to the theoretical value of 1 for a totally reversible reaction [93] . Additionally, we observed a very modest anodic shift in the $E_{1/2}$ value for the CFM-MWCNT/NAF relative to CFM, suggesting a catalytic effect of the MWCNT.

For each electrode tested, the anodic and cathodic peak currents were determined for each scan rate and I_p was plotted as a function of $\nu^{1/2}$. Data was fitted to a linear regression in order to determine the slope. A representative plot is presented in Fig 5. As we can see, the anodic (blue) and cathodic (red) peak currents increased linearly with the square root of the scan rate, indicating that the process is diffusion controlled [87]. Using the Randles-Sevcik equation, the EAS was determined for CFM and CFM-MWCNT/Naf. Despite previous results in other studies showing significant increase in EAS after coating, our results showed no significant change (paired t-student test, P=0.36) as shown in Fig. 6.

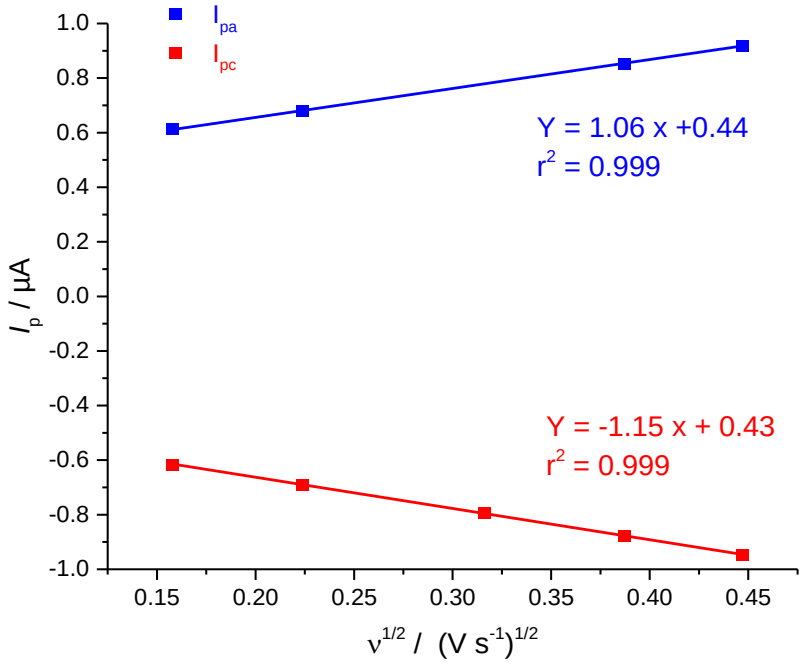

Figure 5. Representative plot of *I*p vs. $\nu^{1/2}$ with the respective equation for the linear fit of each data set.

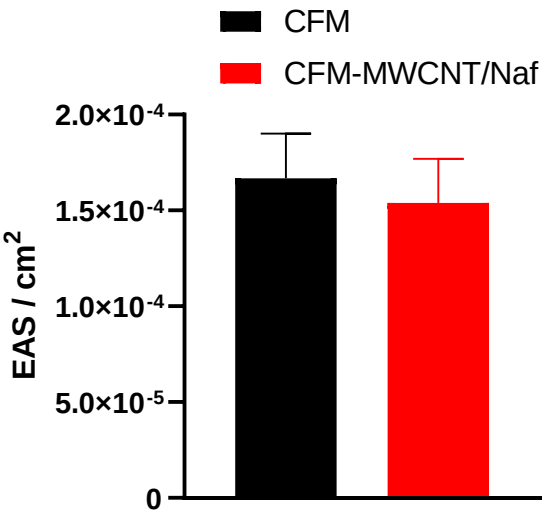

Figure 6. Electrochemical Active Surface determined for CNT and CFM-MWCNT/Naf (N=9). Data represent average ± SEM value for ESA.

3.2. Electrochemical Impedance Spectroscopy

To evaluate the effect of MWCNT- modification on the interface properties of CFM we obtained electrochemical impedance spectrograms from a single CFM before (CFM) and after (CFM-MWCNT/NAF) modification. These were obtained in deoxygenated 0.05M PBS Lite (pH=7.4), applying a 10mV sinusoidal amplitude wave between 100kHz and 0.1 at the open circuit potential (OCP) (vs. Ag/AgCl).

As can be observed from the Bode plots presented in Fig. 7, we observed an increase in the impedance measured at 1 kHz from 3.4 to 3.8 kΩ following coating with MWCNT, being these values still low and fit for *in vivo* recordings, since less energy is required to deliver current to the tissue with a low impedance, ensuring a higher efficiency, decreasing noise in our recordings [50,87]. The same is evident from the Nyquist plots presented in Fig. 8.

By fitting the experimental data from each microelectrode to the equivalent circuit presented in Fig. 9C, we obtained the values for α_1 of 0,78 (CFM) and 0,75 (CFM-MWCNT/NAF). The theoretical value for a smooth surface is $\alpha = 1$, so we can conclude that coating MWCNT alters the surface of the microelectrode, confirming that the nanotubes adhere to the carbon fibre [71]. The equivalent circuit used consists in a cell resistance (R1), combined with a constant phase element (CPE1), parallel with a series combination of a charge transfer resistance and a Warburg impedance element, accounting for mass transfer limitations imposed by diffusion that can appear at lower frequencies, combining with another constant phase element (CPE2) and cell resistance (R3).

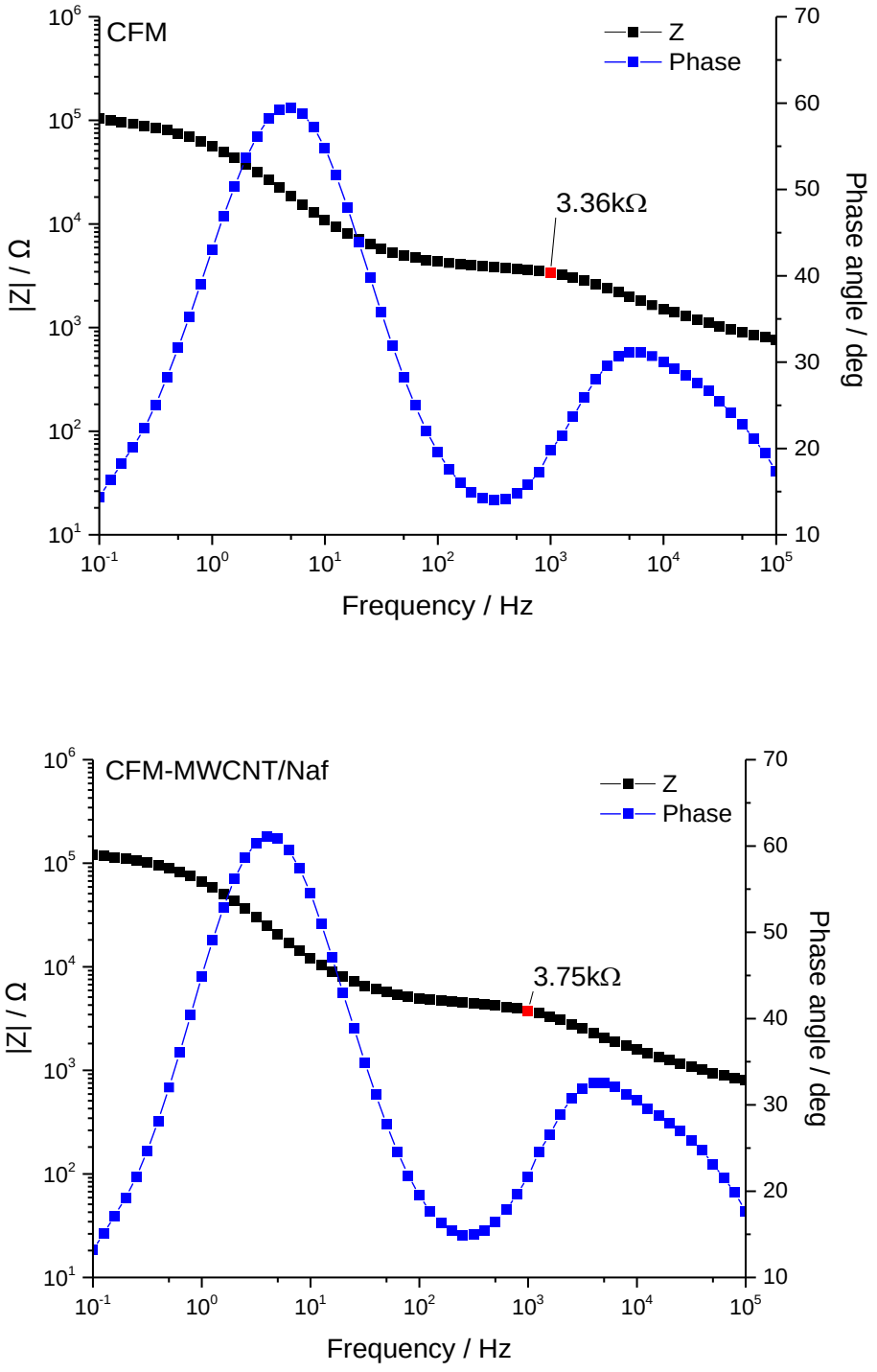

Figure 7. Impedance−frequency (Bode) plots obtained from the same CFM before (top) and after (bottom) coating with MWCNT/Naf. The filled blue squares represent impedance values (|Z|) values while black squares represent phase shift. The red square highlights the |Z| value at 1 kHz.

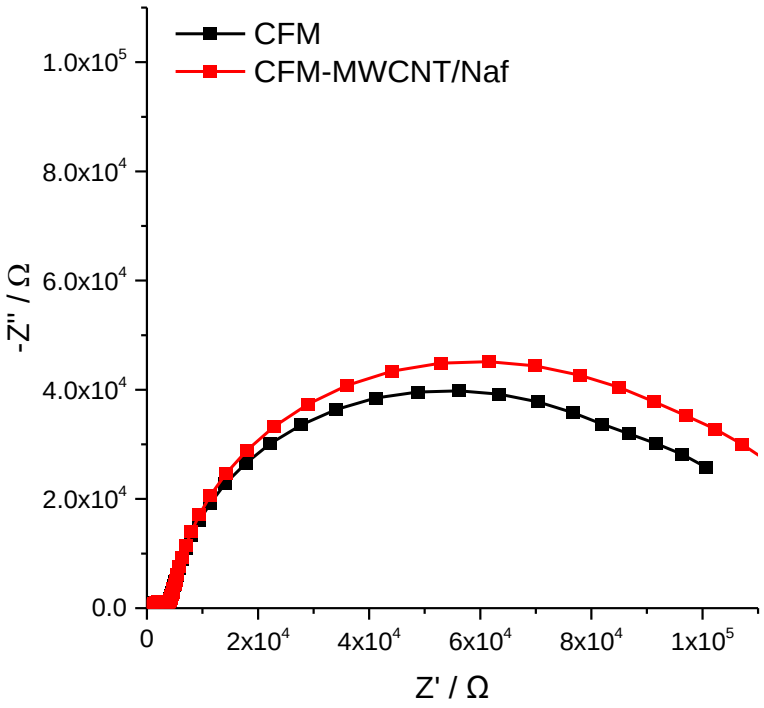

Figure 8. Nyquist plot plots obtained from the same CFM before (black) and after (red) coating with MWCNT.

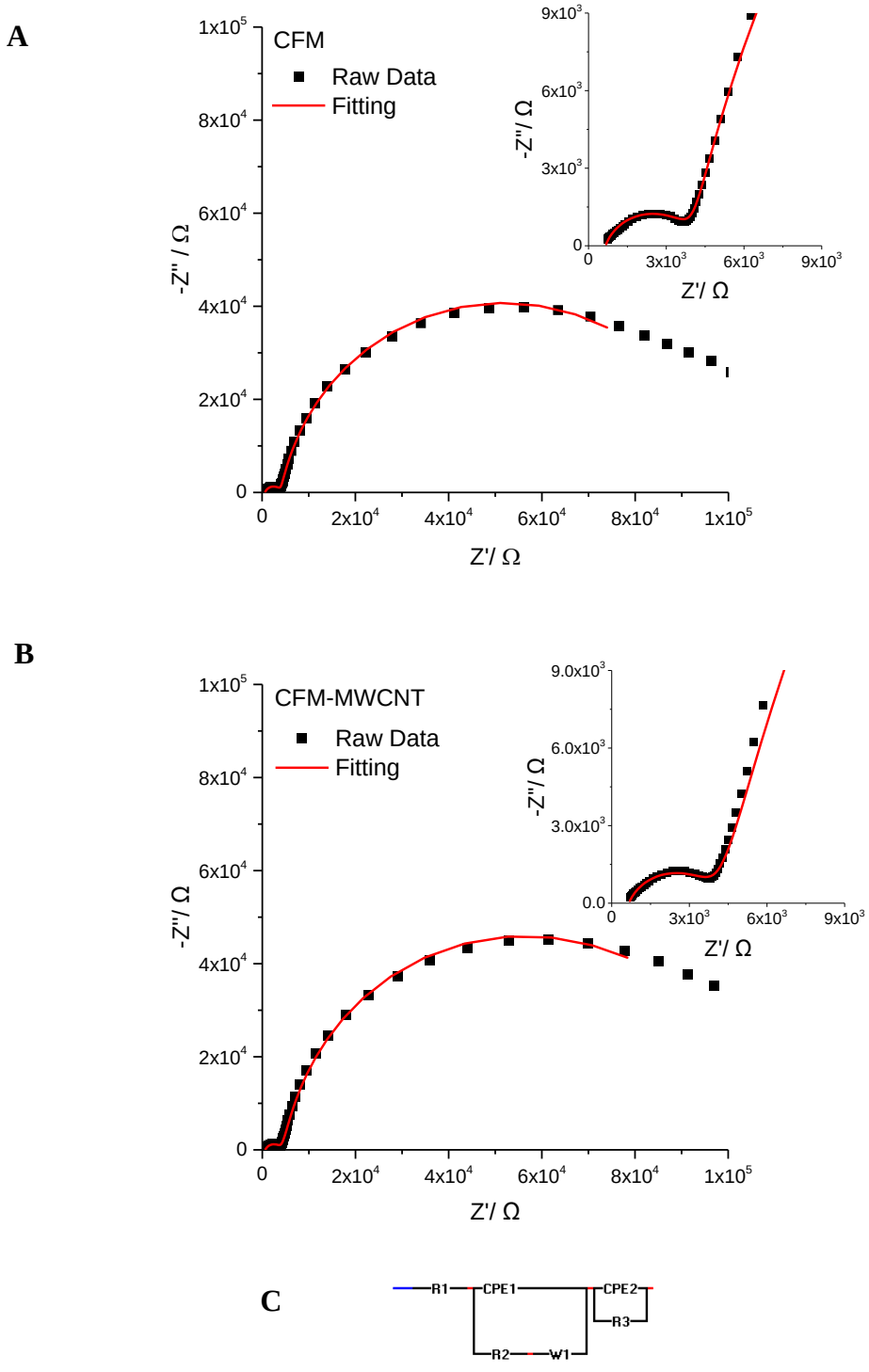

Figure 9. (A and B) Electrochemical impedance spectrum (Nyquist plot) of experimental data for a CFM and CFM-MWCNT/NAF, respectively. The red line shows fitting to the electrical equivalent circuit shown in (B). (B) Equivalent electrical circuits used to fit the impedance spectra.

3.3. Electrocatalytic effect of MWCNT on Oxygen Reduction Reaction

In order to investigate the putative catalytic effect of MWCNT-modification on the O_2 reduction reaction, we obtained cyclic voltammograms in PBS for a CFM before and after coating. As can be observed in Fig. 10, both CFM and CFM-MWCNT/NAF displayed a similar profile in the absence of O_2 (dashed lined). Both types of microelectrodes responded to the presence of O_2 in solution, with a robust reduction current observed. By fitting the cathodic wave to a sigmoidal function, we determined the value of $E_{1/2}$ for each microelectrode and that coating of CFM with MWCNT resulted in an anodic shift in the reduction potential from -0,592 V for the CFM to -0,535 V CFM-MWCNT/NAF. This confirmed the electrocatalytic effect of MWCNT on the O_2 reduction reaction.

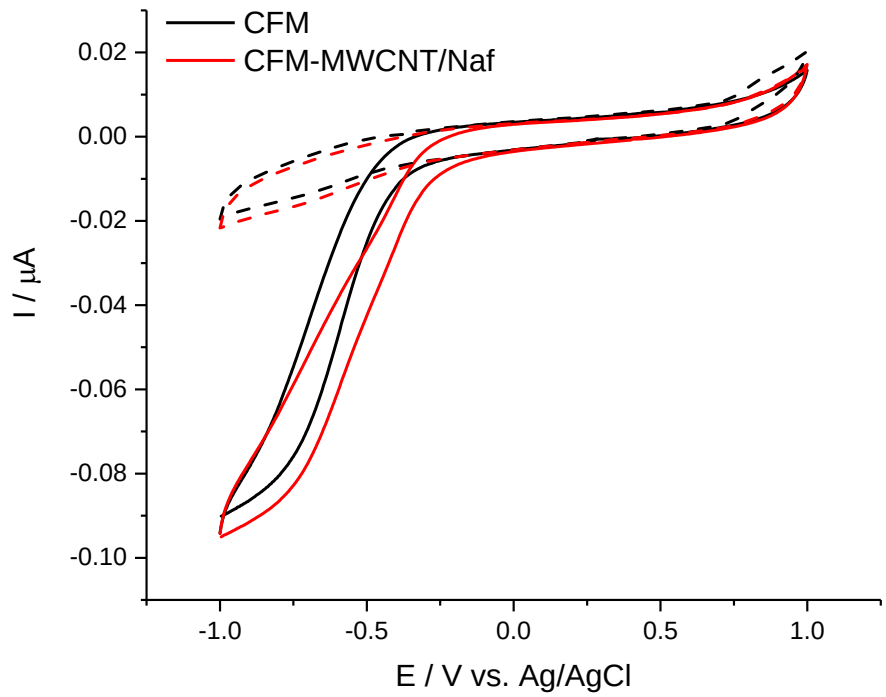

Figure 10. Cyclic voltammogram for CFM (black) and CFM-MWCNT/Naf (red) obtained between -1.0 and +1.0 V vs. Ag/AgCl, at a scan rate of 50 m V s^{-1}. Dashed lines represent voltammograms obtained in N_2 -purged PBS while solid lines were obtained in PBS containing 0,27 mM O_2 [50].

So as to determine the optimal working potential for amperometric monitoring of O_2 *in vivo*, CFM and CFM-MWCNT/NAF were calibrated for O_2 at different working potentials, ranging from -0.2 to -1.0 V. vs. Ag/AgCl. Additionally, to determine the effect of the Nafion® matrix used to deposit the MWCNT on the CFM surface, we repeated this with CFM coated only with Nafion® 0.5% (CFM-Naf). The sensitivity was determined from the slope of each calibration curve obtained and normalized for the maximal slope obtained for -1.0 V vs. Ag/AgCl. As can be observed in Fig. 11, we found that CFM-MWCNT/NAF displayed a significant increase in sensitivity as compared to CFM for working potentials between -0.5 and -0.8 V vs. Ag/AgCl, while for CFM-Naf only for -0.8 V was there a tendency for increased sensitivity compared to CFM.

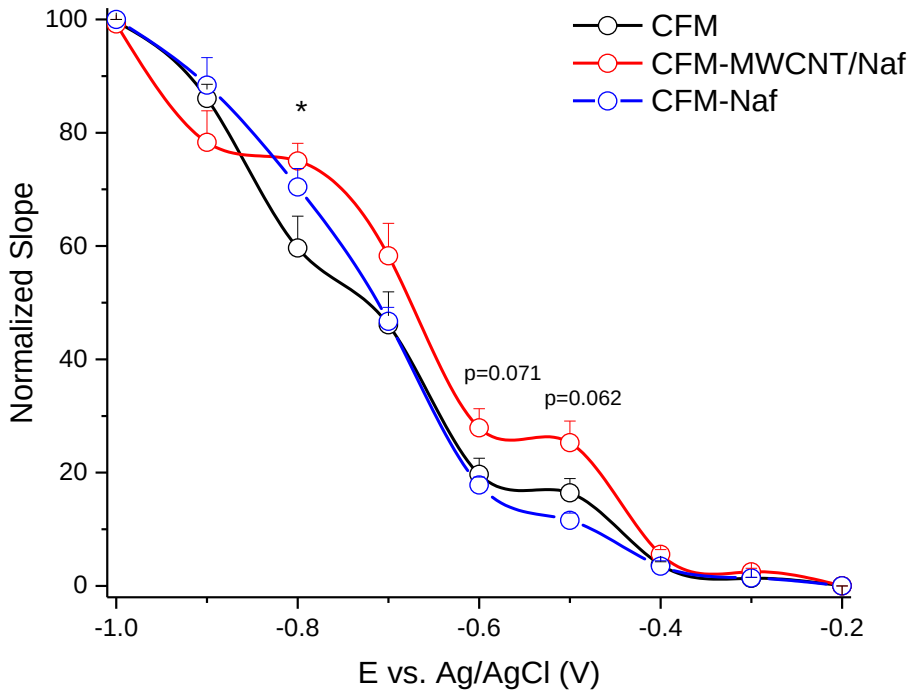

Figure 11. Comparison of the normalized slope obtained from calibration of CFM (black), CFM-MWCNT/NAF (red) and CFM-Naf (blue) at different working potentials ranging from -0.2 to -1.0 V vs. Ag/AgCl. Values represent average ± SEM. * P<0.05 for CFM-MWCNT/NAF vs. CFM, paired t-Student test.

At first look, we are tempted to choose the highest value that this sensitivity boost is noticed which is -0.8V, but previous studies and experiments performed to measure tissue O_2 have been recorded at -0.6V [49,50,87]. In addition, increasing the potential even more means an increase in baseline current and noise [87]. Furthermore, we expect low values of tissue O_2 and the variations that we are expecting are in the µM range [87]. With this in mind, we chose -0.6V vs Ag/AgCl as the optimal applied potential.

The O_2 reduction reaction can follow one of 2 pathways: direct 4-electron reduction to H_2O or a 2-step-2-electron reduction in which H_2O_2 is an intermediate species (Equations 1-3)

$$(1) \quad O_2 + 4H^+ + 4e^- \rightarrow 2H_2O\,, \quad E^0 = 1{,}23V$$

$$(2) \quad O_2 + 2H^+ + 2e^- \rightarrow 2H_2O_2, \quad E^0 = 0{,}67V$$

$$(3) \quad H_2O_2 + 2H^+ + 2e^- \rightarrow 2H_2O, \quad E^0 = 1{,}76V$$

The voltammograms shown above only display one reduction step, meaning that the O_2 reduction reaction occurring at the surface of the CFM is most likely to be the one-step 4-electron reduction reaction to H_2O [50]. On the other hand, from Fig. 11 it appears quite evident that for the CFM-MWCNT/NAF, a 2-step-2-electrode reaction is most like for the O_2 reduction reaction.

In Figure 12, we show a representative calibration recording and the respective calibration curve (inset) of a CFM-MWCNT/NAF at the aforementioned optimal working potential. A linear profile can be observed for the concentration range of 0-50 µM and we obtained a mean value for sensitivity of 0.243$\pm$ 0.060 nA μM^{-1} (N=16).

From the calibration curve were also determined de limit of detection (LOD) using the following expression:

$$LOD = 3 \times SD/m$$

which the SD represents the standard deviation of the baseline and m stands for the slope of the calibration curve [87]. We found a mean LOD value of 2.963 $\pm$ 0.18 µM (N=16)

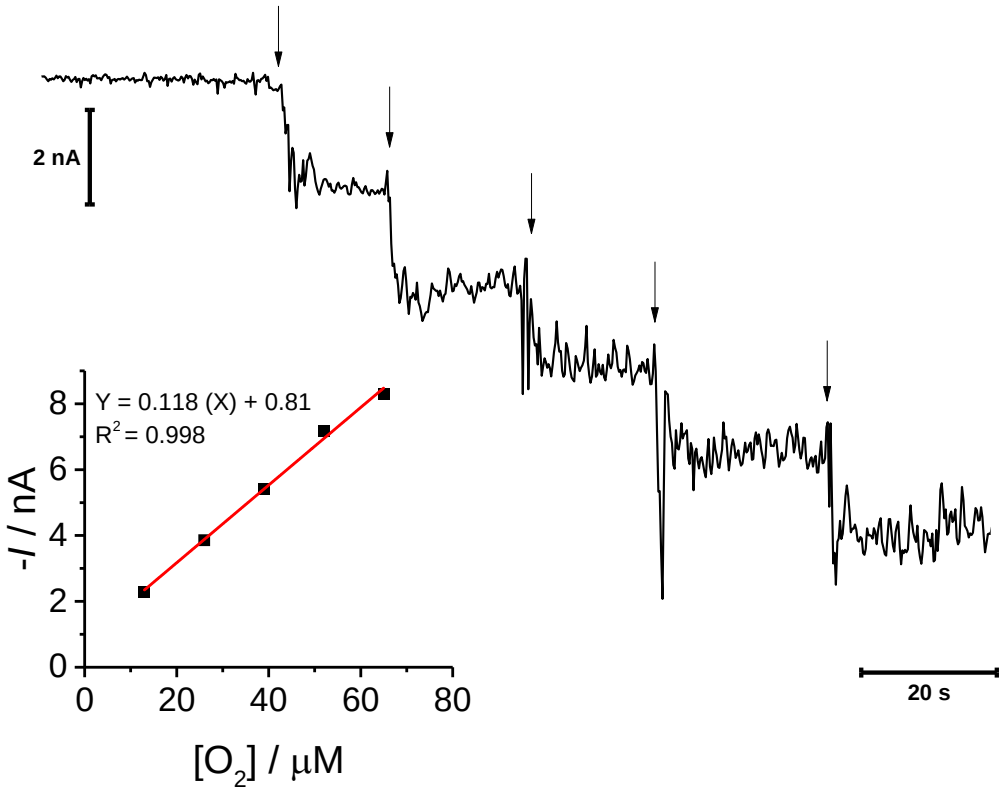

Figure 12. Representative amperometric recording of a calibration of a CFM-MWCNT/NAF at a working potential of -0,6V vs. Ag/AgCl. The arrows indicate the moment of addition of O_2 to the N_2-purged buffer (PBS, pH 7.4). Each addition consisted of 0,2 mL of a saturated O_2 solution, corresponding to incremental increases in O_2 of 13 µM for each addition. Inset is the respective calibration curve.

3.4. Suitability for *in vivo* monitoring of oxygen concentration dynamics in the rodent brain

In order to validate the suitability of CFM-MWCNT/NAF to monitor rapid changes in brain tissue O_2 associated with changes in neural activity, we performed an *in vivo* experiment in the brain of an anesthetized *wistar* rat using a model of local cortical depolarization evoked by high K^+. To this purpose, the CFM-MWCNT/NAF was first coupled to a micropipette in an array, as shown in Fig. 13.

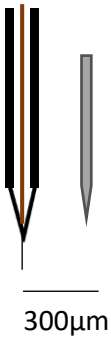

Figure 13. Schematic representation of the array composed by the CFM-MWCNT/Naf (left) and the micropipette (right).

The array comprised of a CFM-MWCNT/NAF, and the micropipette filled with a KCl solution (70 mM) was lowered into the rat cortex (AP=-0,2; ML=1,0; DV=1,5 mm). Once a stable background current was obtained, changes in O_2 were evoked by local depolarization as a result of puff application of KCl (50 nL). This was repeated 4 times (Fig. 14A). For each KCl application we observed a biphasic change in O_2: an initial consumption phase resulted in an average decrease of 2.7 ± 0.34 µM from baseline was followed by a transient increase in O_2 of 18.3 ± 2.8 µM, which corresponds to the hyperaemic phase in which local vasodilation leads to increase O_2 supply to tissue in response to increase activity – neurovascular coupling. With these results we can see that the CFM-MWCNT/NAF produced are recording rapid changes in brain tissue O_2 concentration as expected since previous literature also reports that the KCl induced depolarizations are accompanied by a slight significant increase in tissue pO_2, being noticeable in some experiments a small initial decrease in O_2 levels. This O_2 is demanded by the brain to repolarize the tissue, increasing blood flow [94,95].

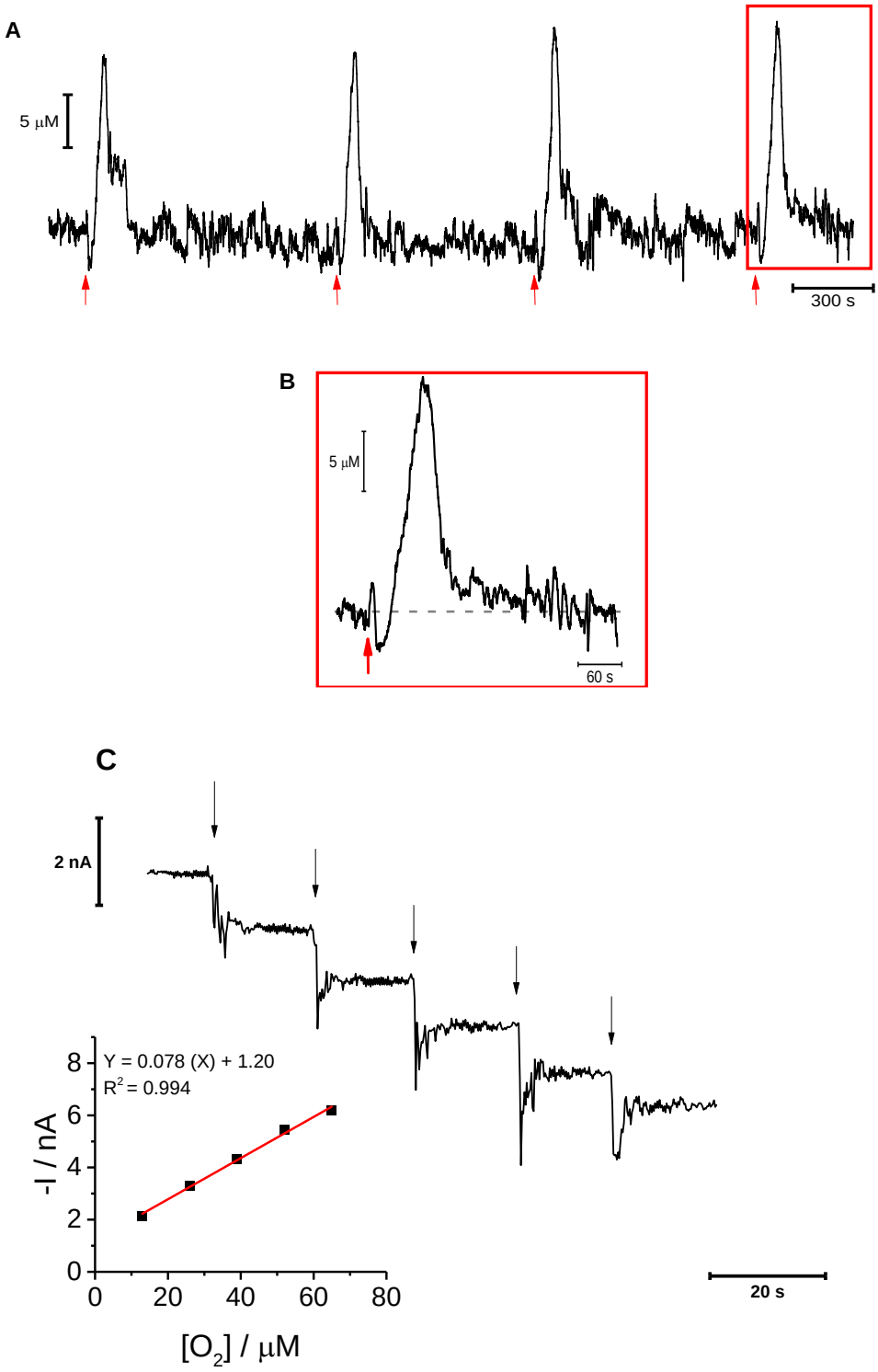

Figure 14. (A) *In vivo* recording of changes in [O_2] in the rat cortex evoked by a puff application of KCl 70 mM (red arrow) (There were 4 applications performed being them of 100, 100, 150 and 150 nL respectively) and (B) shows the detailed view of the individual response marked with a red box in (A). The calibration curve of the

MWCNT-CFM before the experiment is represented in (C) and in inset is the respective calibration curve.

3.5. *In vivo* monitoring of oxygen concentration dynamics during 4-AP evoked seizures

In order to evaluate the changes in brain tissue O_2 associated with seizure activity, we monitored O_2 in the dentate gyrus (DG) of the hippocampus and evoked a seizure by local application of 4-AP. To this purpose, an array comprising a CFM-MWCNT/NAF, and a micropipette filled in 4-AP (25 mM) was lowered into the brain of anesthetized wistar rats. Once a stable background current was obtained, a seizure was evoked by local application of 4-AP. We performed 3 individual experiments on 3 different animals, which are now described in detail. In all cases, the amperometric current was recorded at an acquisition frequency of 40 Hz, to allow the monitoring of both electrochemical (<1Hz) data and local field potential related currents (>1 Hz) [8].

3.5.1. Experiment 1

In this first experiment, the CFM-MWCNT/NAF was placed in the DG (AP=-4.2; ML=2.4; DV=-3.5 mm) and 4-AP was administered during the period shown by the grey-filled box in Fig. 15A. As can be observed, following 4-AP administration, the O_2 concentration dropped rapidly. Following approximately 250 s of 4-AP, a sharp transient decrease in O_2 was observed, that coincided with increase in power observed in the spectrogram. This profile was repeated two more times following which increased power was accompanied by two bi-phasic changes in O_2, with an increase above baseline following the initial consumption phase. This surplus in O_2 in brain tissue is typically the result of hyperaemia – an increase in cerebral blood flow in response to a stimulus that results in flux of nutrients beyond tissue demand.

In Fig. 15B we can observe a more detailed view of the region highlighted with a red box in Fig. 15B. The top recording shows the low frequency component (a), the middle panel the high frequency component (b) and the bottom panel the corresponding power spectrogram. It is interesting to observed that i) for all events, the decay in O_2

precedes the observed change in the local field potential related current; ii) the profile of the ictal events changes between the mono phasic and the bi-phasic O_2 signals.

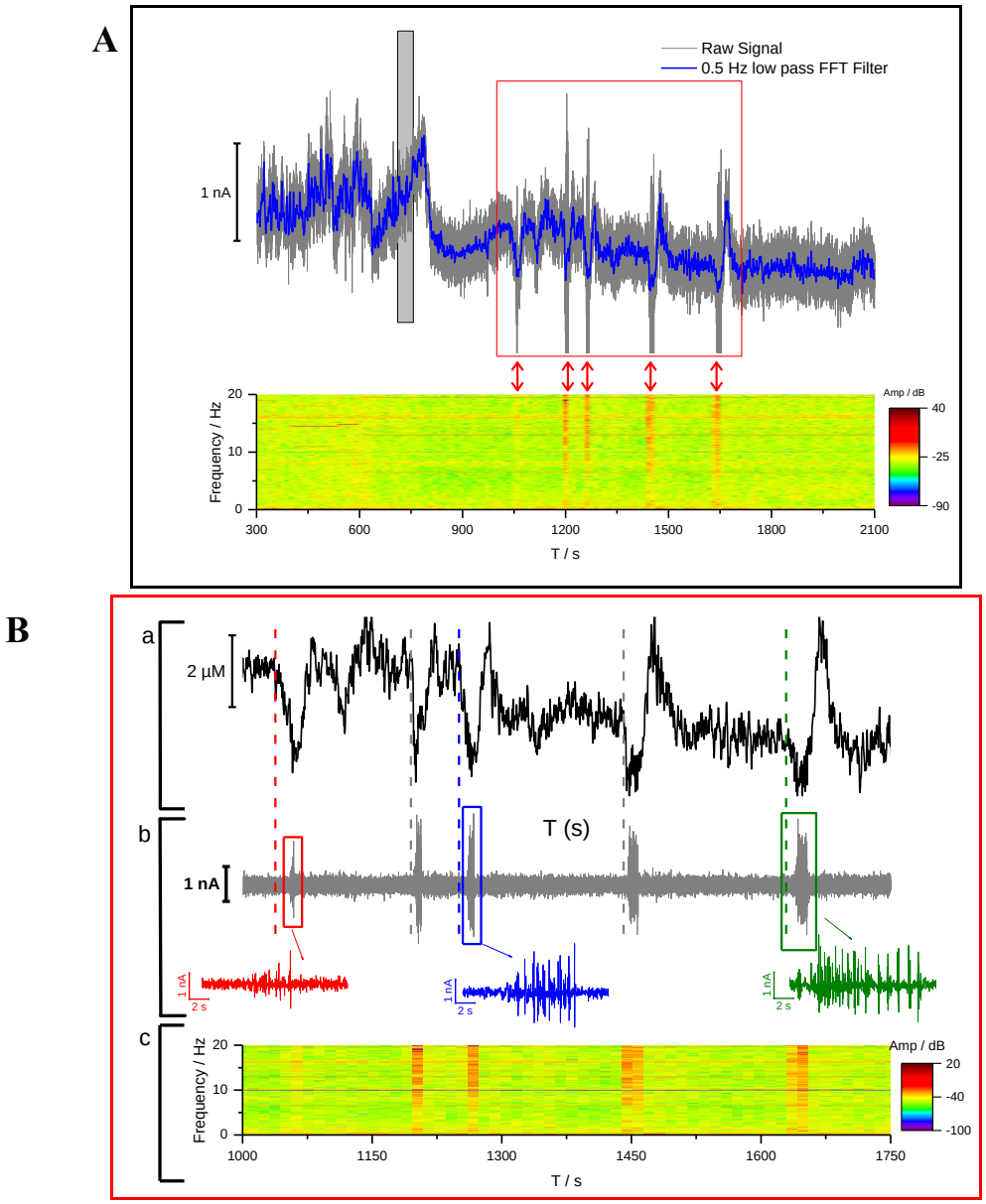

Figure 15. Experiment 1 - Fast sampling (40Hz) amperometric recording of O_2 using a CFM-MWCNT/NAF placed in the hippocampal DG region upon 4-AP induction of seizure. **(A)** Top panel shows the raw signal (grey) and the low pass FFT filter (0.5Hz) (blue) while the bottom panel shows the power spectrum analysis of the high-frequency component. Grey box indicates moment of 4-AP application. Red arrows show ictal events accompanied by changes in pO_2. **(B)** Highlight of the boxed area in A: **a)** low frequency component (O_2); **b)** high frequency component, and **c)** power spectrogram.

Dashed vertical lines indicate moment of change in O_2. The insets in panel **b** are blowouts of the boxed areas in the high frequency component.

As observed before with the KCl administrations, we can notice a biphasic change in response to the 4-aminopyridin application on the last 2 spikes recorded, having a consumption of O_2 in the first place of about 1.68 ± 0.23 µM, followed by an increase around 4.92 ± 0.16 µM, ending on a return to the baseline. As for the other 3 previous spikes we can perceive a consume of about 2.97 ± 0.26 µM. Also, we can see that there is a small reduction in O_2 concentration, comparing before and after the chemoconvulsant addition of about 3.39 µM. Next, we can see a detailed view of the individual spikes separately in figure 16:

3.5.2. Experiment 2

In a second experiment, the CFM-MWCNT/NAF was placed in the dentate gyrus (AP=-3.7; ML=1.9; DV=-2.3 mm). 4-amynopyridine was administered in a large quantity to promote the SE, resulting in seizure activity as shown in Fig. 16 A. As compared to experiment 1 where only sparse ictal discharges were observed, in experiment 2 we observed longer bursting periods, clearly evident by the repetitive increase in power observed in the power spectrogram in Fig. 16 A, panel c. We can also clearly observe the theta waves that are characteristic of an epileptic episode in which the onset of SE is preceded by a period of theta wave synchronization, accompanied by a prolonged period of increased power in all frequencies [3,8,96]. We also observed from the second burst onward the appearance of hypersynchrony waves at the beginning of the burst and then become diffuse.

From the second burst onward, we observed that the onset of the burst was accompanied by a sharp decrease in O_2, highlighted with red asterisks in Fig 16B. During the burst, O_2 tended to stabilize and during the inter-burst period, an increase in O_2 was observed (green asterisks) followed by a slow decrease until the sharp decrease in O_2 was observed at the beginning of the subsequent burst. This is more clearly observed in Figure 17.

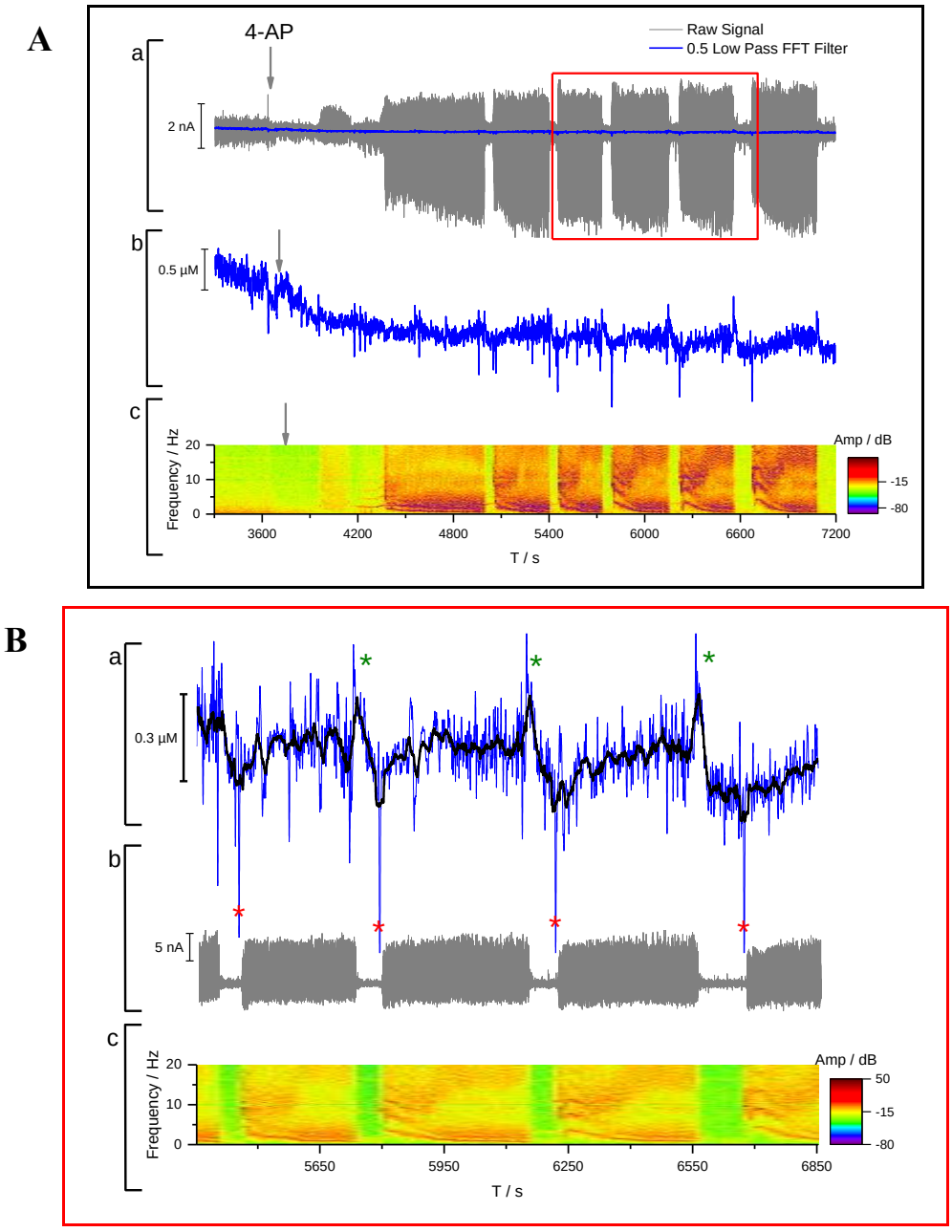

Figure 16. Experiment 2 - (A) Top panel (a) shows the raw signal recorded at 40 Hz in grey and in blue the 0.5 Hz low pass filter. Panel b shows and amplified view of the low frequency component of the signal and panel c is the respective power spectrogram. Arrows indicate moment of 4-AP application. (B) Highlight of boxed area in A. In panel a, the blue trace represents the low frequency component (O_2), while black trace represents the 400-point moving average of the low frequency component, to highlight

slower changes in pO_2. Panel b shows the high frequency component and panel c the respective power spectrogram.

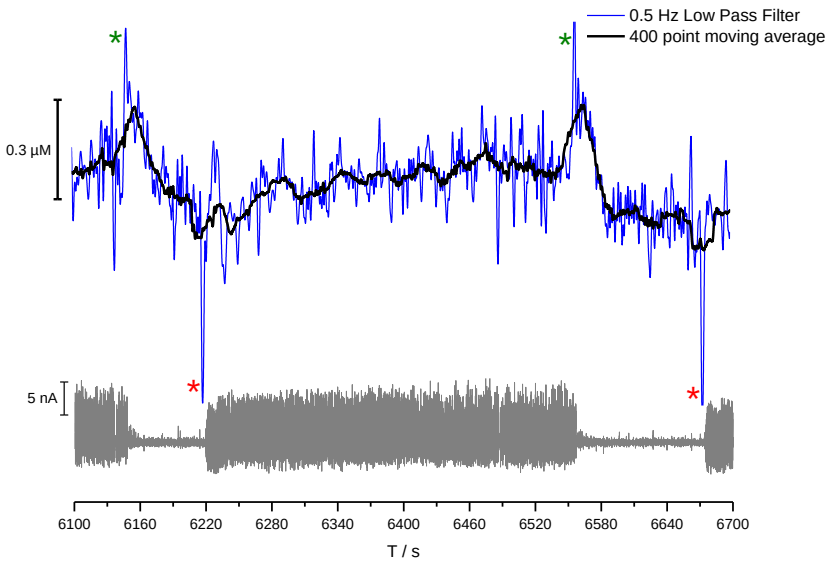

Figure 17. Experiment 2 – Detailed view of the low frequency (top) and high-frequency (bottom) components of burst 3 in experiment 2

3.5.3. Experiment 3

In the third experiment, application of 4-AP resulted in burst-like discharges, as shown in Figure 18. Similarly, to the previous 2 recording, each discharge was accompanied by a decrease in pO_2 (0.27 ± 0.06 µM) followed by a return to the baseline. No evident hyperoxia was observed in this particular recording. In this experiment it is also possible to visualize the theta waves that precede a period of SE, followed by a prolonged period of increased power in all frequencies.

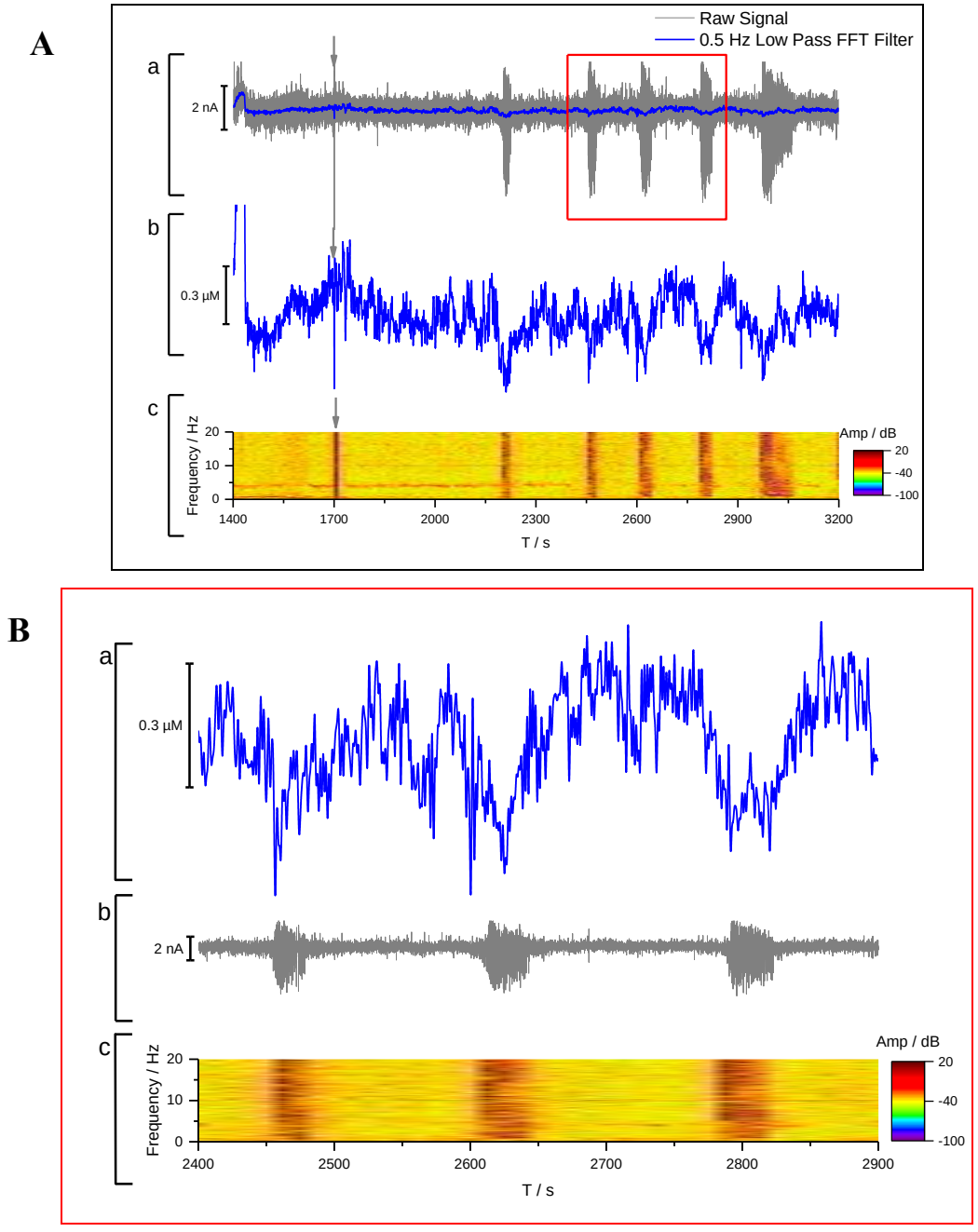

Figure 18. Experiment 3. (A) Top panel (a) shows the raw signal recorded at 40 Hz in grey and in blue the 0.5 Hz low pass filter. Panel b shows and amplified view of the low frequency component of the signal and panel c is the respective power spectrogram. Arrows indicate moment of 4-AP application. (B) Highlight of boxed area in A. In panel a, the blue trace represents the low frequency component (O_2), while black trace represents the 400-point moving average of the low frequency component, to highlight slower changes in pO_2. Panel b shows the high frequency component and panel c the respective power spectrogram.

4. DISCUSSION

Our current understanding of brain activity, both in physiology and pathophysiology, holds to gain from concurrent monitoring of neurochemical and electrophysiological activity. This has been attempted in different forms, either using an individual recording electrode for each modality, or a single electrode alternating between electrochemical and electrophysiological monitoring [29]. The pivotal work by the group of Nicolelis demonstrated the electrochemical signal recorded at high frequency of acquisition carried both the neurochemical information in the low frequency component (< 1Hz) as well as electrophysiological information in the form of local field potential related currents in the high frequency component (> 1Hz) [8].

Such concurrent monitoring becomes increasing interesting in the context of epilepsy, since seizures display both aberrant neurophysiological activity and acute or prolonged changes in neurochemicals including neurotransmitters and neurometabolic markers such as oxygen, glucose, and lactate [3,25,28,29,35]. Monitoring interstitial oxygen is of particular interest, since changes in its concentration reflect the balance between consumption by cells, mainly for energy production, and delivery through circulation. While the increase in neuronal activity observed during a seizure imposes and acute increase in energy demand which leads to a rapid consumption of oxygen, local cerebral blood flow increases in response, resulting in a delayed hyperaemic phase where oxygen delivery exceeds tissue requirements [3]. Indeed, functional neuroimaging techniques explore the hemodynamic response as a surrogate signal of neuronal activity [33,54,55]. Considering this, design of novel tools for concurrent monitoring of brain tissue oxygen and electrophysiology is of great interest in the context of pre-clinical epilepsy research and may hold potential for translation to clinical research.

Electrochemical monitoring of oxygen has classically used Pt based electrodes, which display excellent electroanalytical properties towards the oxygen reduction reaction [3,8,87]. However, carbon-based electrodes may be an interesting alternative, in particular due to reduced cost. Carbon fibre microelectrodes can be constructed with small carbon filaments (as low as 5 µm in diameter) which introduce minimal damage when inserted in brain tissue [97]. The poorer electroanalytical performance of carbon relative

to platinum for oxygen reduction can be mitigated using carbon nanotubes, which have been described to enhance sensor performance [6].

In this project, we designed, evaluated and validated CFM modified by coating with MWCNT in a Nafion® matrix for concurrent monitoring of brain tissue oxygen in a pre-clinical model of seizures. In particular, individual CFM were coated with MWCNT by dipping the electrode tip into a suspension of MWCNT (10 mg mL^{-1}) in Nafion 0.5 % followed by drying at 180 ºC. Evaluation of the electroactive surface area of the CFM before and after coating revealed that very little material was deposited on the carbon fibre surface. A putative strategy to increase CNT load would be to repeat the coating process two or three more times. Other studies using CFM coated with SWCNT and MWCNT in 0.5% Nafion using a dipping strategy similar to the one used here used a 100 mg mL^{-1} suspension, which could optimize the adherence of the nanotubes to the carbon fibre [6,98]. Deposition of MWCNT has been shown to increase the ESA in BSCF-based electrodes or identical metallic interdigitated electrodes, while also displaying catalytic activity towards the electrochemical O_2 reduction [99,100].

Electrochemical impedance spectroscopy revealed an increment on the impedance of the coated microelectrodes. Furthermore, fitting of the experimental data to an equivalent circuit confirmed the presence of deposited MWCNT on the CFM active surface. Other studies comparing several impedances have shown a noticeable decrease in impedance, when comparing CFMs with CNT fibres that can be explained by the high surface area that the CNTs grant [101]. In our studies, this area does not increase with the coating, which can then originate a different outcome for these results to those suggested by other investigations.

Most interestingly, we found that even for such a low load of MWCNT, they did improve the electroanalytical performance of the CFM towards the oxygen reduction reaction, displayed as a decrease in the overpotential required for O_2 monitoring and increased sensitivity between -0.6 and -0.8 V vs. Ag/AgCl, which has also been described by others [87,100,102,103].

Adding CNTs to several biosensors and devices is reported in literature to possess a significative effect in improving the sensitivity of the devices, not only towards oxygen measures, but also towards ascorbate, dopamine, adenosine, and others [103–106]. As for

the cyclic voltammetry studies, it was possible to notice the electrocatalytic effect towards the reduction of O_2 that the MWCNTs provide as previous studies report [104]. In CFMs altered with SWCNT or MWCNT, a negative shift on the oxidation of ascorbate peak was observed [6]. Furthermore, the electrocatalytic effect that CNT add to microelectrodes was also displayed in studies of the oxidation of ascorbate [6,98]. Similarly, for the oxidation of dopamine an electrocatalytic effect was noticeable upon the application of the nanotubes to the electrode [107].

The first *in vivo* experiment, performed with KCl administration has shown that the CFM-MWCNT/NAF was capable and suited for the monitorization of rapid changes on O_2 concentrations, which goes in accordance with what was expected for the KCl depolarization, meaning that these electrodes make a good analytical tool for *in vivo* oximetry.

For our experiments with 4-AP, the CFM-MWCNT/Naf were able to record variations of tissue pO_2 and local field potential related currents during seizures in the hippocampus of anesthetized rats, as was achieved in previous studies [3,8] . Choline and oxygen variations were possible to be measured simultaneously as local field potentials, but without using the same type of electrodes present on this study, meaning that CFM-MWCNT/NAF constitute a good approach to achieve this type of measurements [3,8]. In these experiments, two different profiles of reaction to the chemoconvulsant stimulus were obtained, as proved by the spiking profile that was different in one of the experiments. In addition, and by analysing the STFT, there was a significative difference in the duration of the seizures for one of the experiments. Additionally, it was possible to observe the epileptic dip on one of the recordings, which could be justified by several factors, since different methodologies, anaesthesia, degree of oxygenation, and species may be responsible for this event [108]. Moreover, the extent of the amplitude of this initial dip can be influenced by anaesthesia and blood oxygen level, which we did not monitor [108]. To infer on how this animal model responds to the chemoconvulsant, more experiments on the subject must be conducted in order to reach a more certain and statistically valuable conclusion.

CONCLUSIONS

In this work, we have fabricated in-house CFM, and modified the active surface with a composite film of Nafion® and MWCNTs to improve their analytical performance towards O_2 *in vivo* monitoring in the intact rat brain. The electrochemical characterization and *in vitro* evaluation were performed by using electrochemical techniques such cyclic voltammetry and EIS to assess the ESA and the electrocatalytic effect on oxygen reduction reaction. The ultimate goal was to monitor oxygen concentration dynamics in vivo during seizures evoked by local application of 4-AP.

The results support the following conclusions:

- Coating CFM with a composite film of Nafion and MWCNT does not change ESA significantly.
- EIS studies indicate that MWCNT slightly increase CFM impedance.
- An electrocatalytic effect on the oxygen reduction reaction is observed with MWCNTs, being noticeable an anodic shift in the reduction potential.
- Coating CFMs with Nafion/MWCNT significantly increases the sensitivity, when compared to bare CFM for working potentials between -0.5 and -0.8 V vs. Ag/AgCl.
- Modified CFM are capable of recording rapid changes in brain tissue O_2 concentration.
- Concurrent measurements of pO_2 and local filed potential-related currents can be obtained by high sampling amperometry with a single sensor CFM-MWCNT/Naf.
- A key feature of *status epilepticus* is rhythmic electrical activity with different spiking profiles accompanied by O_2 fluctuations.
- A period of theta wave synchronization preceding the onset of SE, followed by a prolonged period of increased power in all frequencies.

REFERENCES

[1] M. Ihle, H. Feldwisch-Drentrup, C.A. Teixeira, A. Witon, B. Schelter, J. Timmer, A. Schulze-Bonhage, EPILEPSIAE – A European epilepsy database, Comput Methods Programs Biomed. 106 (2012) 127–138. https://doi.org/10.1016/j.cmpb.2010.08.011.

[2] G. Curia, D. Longo, G. Biagini, R.S.G. Jones, M. Avoli, The pilocarpine model of temporal lobe epilepsy, J Neurosci Methods. 172 (2008) 143–157. https://doi.org/10.1016/j.jneumeth.2008.04.019.

[3] A. Ledo, C.F. Lourenço, J. Laranjinha, G.A. Gerhardt, R.M. Barbosa, Combined in Vivo Amperometric Oximetry and Electrophysiology in a Single Sensor: A Tool for Epilepsy Research, Anal Chem. 89 (2017) 12383–12390. https://doi.org/10.1021/acs.analchem.7b03452.

[4] W.O. Tatum, Mesial Temporal Lobe Epilepsy, Journal of Clinical Neurophysiology. 29 (2012) 356–365. https://doi.org/10.1097/WNP.0b013e31826b3ab7.

[5] M.L. Huffman, B.J. Venton, Carbon-fiber microelectrodes for in vivo applications, Analyst. 134 (2009) 18–24. https://doi.org/10.1039/B807563H.

[6] N.R. Ferreira, A. Ledo, J. Laranjinha, G.A. Gerhardt, R.M. Barbosa, Simultaneous measurements of ascorbate and glutamate in vivo in the rat brain using carbon fiber nanocomposite sensors and microbiosensor arrays, Bioelectrochemistry. 121 (2018) 142–150. https://doi.org/10.1016/j.bioelechem.2018.01.009.

[7] L. Agüí, P. Yáñez-Sedeño, J.M. Pingarrón, Role of carbon nanotubes in electroanalytical chemistry, Anal Chim Acta. 622 (2008) 11–47. https://doi.org/10.1016/j.aca.2008.05.070.

[8] H. Zhang, S.-C. Lin, M.A.L. Nicolelis, Acquiring local field potential information from amperometric neurochemical recordings, J Neurosci Methods. 179 (2009) 191–200. https://doi.org/10.1016/j.jneumeth.2009.01.023.

[9] R.S. Fisher, W. van E. Boas, W. Blume, C. Elger, P. Genton, P. Lee, J. Engel, Epileptic Seizures and Epilepsy: Definitions Proposed by the International League Against Epilepsy (ILAE) and the International Bureau for Epilepsy (IBE), Epilepsia. 46 (2005) 470–472. https://doi.org/10.1111/j.0013-9580.2005.66104.x.

[10] S.N. Rakhade, F.E. Jensen, Epileptogenesis in the immature brain: emerging mechanisms, Nat Rev Neurol. 5 (2009) 380–391. https://doi.org/10.1038/nrneurol.2009.80.

[11] R.S. Fisher, C. Acevedo, A. Arzimanoglou, A. Bogacz, J.H. Cross, C.E. Elger, J. Engel, L. Forsgren, J.A. French, M. Glynn, D.C. Hesdorffer, B.I. Lee, G.W. Mathern, S.L. Moshé, E. Perucca, I.E. Scheffer, T. Tomson, M. Watanabe, S. Wiebe, ILAE Official Report: A practical clinical definition of epilepsy, Epilepsia. 55 (2014) 475–482. https://doi.org/10.1111/epi.12550.

[12] N. Granger, P. Convers, O. Beauchet, D. Imler, A. Viallon, B. Laurent, D. Michel, [First epileptic seizure in the elderly: electroclinical and etiological data in 341 patients]., Rev Neurol (Paris). 158 11 (2002) 1088–95.

[13] S. Mlinar, Z. Rener Primec, D. Petek, Psychosocial Factors in the Experience of Epilepsy: A Qualitative Analysis of Narratives, Behavioural Neurology. 2021 (2021) 1–9. https://doi.org/10.1155/2021/9976110.
[14] J.A. French, P.D. Williamson, V.M. Thadani, T.M. Darcey, R.H. Mattson, S.S. Spencer, D.D. Spencer, Characteristics of medial temporal lobe epilepsy: I. Results of history and physical examination, Ann Neurol. 34 (1993) 774–780. https://doi.org/10.1002/ana.410340604.
[15] Z. Chen, M.J. Brodie, D. Liew, P. Kwan, Treatment Outcomes in Patients With Newly Diagnosed Epilepsy Treated With Established and New Antiepileptic Drugs, JAMA Neurol. 75 (2018) 279. https://doi.org/10.1001/jamaneurol.2017.3949.
[16] P. Czapinski, B. Blaszczyk, S. Czuczwar, Mechanisms of Action of Antiepileptic Drugs, Curr Top Med Chem. 5 (2005) 3–14. https://doi.org/10.2174/1568026053386962.
[17] K.D. Laxer, E. Trinka, L.J. Hirsch, F. Cendes, J. Langfitt, N. Delanty, T. Resnick, S.R. Benbadis, The consequences of refractory epilepsy and its treatment, Epilepsy & Behavior. 37 (2014) 59–70. https://doi.org/10.1016/j.yebeh.2014.05.031.
[18] P. Kwan, A. Arzimanoglou, A.T. Berg, M.J. Brodie, W. Allen Hauser, G. Mathern, S.L. Moshé, E. Perucca, S. Wiebe, J. French, Definition of drug resistant epilepsy: Consensus proposal by the ad hoc Task Force of the ILAE Commission on Therapeutic Strategies, Epilepsia. 51 (2009) 1069–1077. https://doi.org/10.1111/j.1528-1167.2009.02397.x.
[19] S. Noachtar, I. Borggraefe, Epilepsy surgery: A critical review, Epilepsy & Behavior. 15 (2009) 66–72. https://doi.org/10.1016/j.yebeh.2009.02.028.
[20] O. Devinsky, W.B. Barr, B.G. Vickrey, A.T. Berg, C.W. Bazil, S. v. Pacia, J.T. Langfitt, T.S. Walczak, M.R. Sperling, S. Shinnar, S.S. Spencer, Changes in depression and anxiety after resective surgery for epilepsy, Neurology. 65 (2005) 1744–1749. https://doi.org/10.1212/01.wnl.0000187114.71524.c3.
[21] K. Vonck, P. Boon, D. Roost, Anatomical and physiological basis and mechanism of action of neurostimulation for epilepsy, in: Operative Neuromodulation, Springer Vienna, Vienna, n.d.: pp. 321–328. https://doi.org/10.1007/978-3-211-33081-4_35.
[22] C.E. Stafstrom, Dietary Approaches to Epilepsy Treatment: Old and New Options on the Menu, Epilepsy Curr. 4 (2004) 215–222. https://doi.org/10.1111/j.1535-7597.2004.46001.x.
[23] S. Schaeffer, C. Iadecola, Revisiting the neurovascular unit, Nat Neurosci. 24 (2021) 1198–1209. https://doi.org/10.1038/s41593-021-00904-7.
[24] C.F. Lourenço, A. Ledo, R.M. Barbosa, J. Laranjinha, Neurovascular-neuroenergetic coupling axis in the brain: master regulation by nitric oxide and consequences in aging and neurodegeneration, Free Radic Biol Med. 108 (2017) 668–682. https://doi.org/10.1016/j.freeradbiomed.2017.04.026.
[25] M.P. Bordone, M.M. Salman, H.E. Titus, E. Amini, J. v. Andersen, B. Chakraborti, A. v. Diuba, T.G. Dubouskaya, E. Ehrke, A. Espindola de Freitas, G. Braga de Freitas, R.A. Gonçalves, D. Gupta, R. Gupta, S.R. Ha, I.A. Hemming, M. Jaggar, E. Jakobsen, P. Kumari, N. Lakkappa, A.P.L. Marsh, J. Mitlöhner, Y. Ogawa, R.K. Paidi, F.C. Ribeiro, A. Salamian, S. Saleem, S.

Sharma, J.M. Silva, S. Singh, K. Sulakhiya, T.W. Tefera, B. Vafadari, A. Yadav, R. Yamazaki, C.I. Seidenbecher, The energetic brain – A review from students to students, J Neurochem. 151 (2019) 139–165. https://doi.org/10.1111/jnc.14829.

[26] C. Iadecola, The Neurovascular Unit Coming of Age: A Journey through Neurovascular Coupling in Health and Disease, Neuron. 96 (2017) 17–42. https://doi.org/10.1016/j.neuron.2017.07.030.

[27] T.H. Schwartz, Neurovascular Coupling and Epilepsy: Hemodynamic Markers for Localizing and Predicting Seizure Onset, Epilepsy Curr. 7 (2007) 91–94. https://doi.org/10.1111/j.1535-7511.2007.00183.x.

[28] C.F. Lourenço, A. Ledo, G.A. Gerhardt, J. Laranjinha, R.M. Barbosa, Neurometabolic and electrophysiological changes during cortical spreading depolarization: multimodal approach based on a lactate-glucose dual microbiosensor arrays, Sci Rep. 7 (2017) 6764. https://doi.org/10.1038/s41598-017-07119-6.

[29] A. Ledo, C.F. Lourenço, J. Laranjinha, G.A. Gerhardt, R.M. Barbosa, Concurrent measurements of neurochemical and electrophysiological activity with microelectrode arrays: New perspectives for constant potential amperometry, Curr Opin Electrochem. 12 (2018) 129–140. https://doi.org/10.1016/j.coelec.2018.05.018.

[30] M. Zhao, J. Nguyen, H. Ma, N. Nishimura, C.B. Schaffer, T.H. Schwartz, Preictal and Ictal Neurovascular and Metabolic Coupling Surrounding a Seizure Focus, Journal of Neuroscience. 31 (2011) 13292–13300. https://doi.org/10.1523/JNEUROSCI.2597-11.2011.

[31] C.A. Ramírez-Fuentes, V. Barrera-Figueroa, B. Tovar-Corona, M.A. Silva-Ramírez, L.I. Garay-Jiménez, Epileptic focus location in the cerebral cortex using linear techniques and complex networks, Nonlinear Dyn. 104 (2021) 2687–2710. https://doi.org/10.1007/s11071-021-06418-y.

[32] M. Zhao, M. Suh, H. Ma, C. Perry, A. Geneslaw, T.H. Schwartz, Focal Increases in Perfusion and Decreases in Hemoglobin Oxygenation Precede Seizure Onset in Spontaneous Human Epilepsy, Epilepsia. 48 (2007) 2059–2067. https://doi.org/10.1111/j.1528-1167.2007.01229.x.

[33] V. Osharina, E. Ponchel, A. Aarabi, R. Grebe, F. Wallois, Local haemodynamic changes preceding interictal spikes: A simultaneous electrocorticography (ECoG) and near-infrared spectroscopy (NIRS) analysis in rats, Neuroimage. 50 (2010) 600–607. https://doi.org/10.1016/j.neuroimage.2010.01.009.

[34] J.W. Pan, A. Williamson, I. Cavus, H.P. Hetherington, H. Zaveri, O.A.C. Petroff, D.D. Spencer, Neurometabolism in human epilepsy, Epilepsia. 49 (2008) 31–41. https://doi.org/10.1111/j.1528-1167.2008.01508.x.

[35] K. Kobow, S. Auvin, F. Jensen, W. Löscher, I. Mody, H. Potschka, D. Prince, A. Sierra, M. Simonato, A. Pitkänen, A. Nehlig, J.M. Rho, Finding a better drug for epilepsy: Antiepileptogenesis targets, Epilepsia. 53 (2012) 1868–1876. https://doi.org/10.1111/j.1528-1167.2012.03716.x.

[36] J. Weaver, K. Liu, In vivo electron paramagnetic resonance oximetry and applications in the brain, Med Gas Res. 7 (2017) 56. https://doi.org/10.4103/2045-9912.202911.

[37] M.E. Watts, R. Pocock, C. Claudianos, Brain Energy and Oxygen Metabolism: Emerging Role in Normal Function and Disease, Front Mol Neurosci. 11 (2018). https://doi.org/10.3389/fnmol.2018.00216.

[38] M.E. Raichle, D.A. Gusnard, Appraising the brain's energy budget, Proceedings of the National Academy of Sciences. 99 (2002) 10237–10239. https://doi.org/10.1073/pnas.172399499.
[39] W.G. LENNOX, OXYGEN SATURATION OF THE ARTERIAL BLOOD IN EPILEPSY, Arch Neurol Psychiatry. 35 (1936) 1198. https://doi.org/10.1001/archneurpsyc.1936.02260060040002.
[40] C. Huneau, H. Benali, H. Chabriat, Investigating Human Neurovascular Coupling Using Functional Neuroimaging: A Critical Review of Dynamic Models, Front Neurosci. 9 (2015). https://doi.org/10.3389/fnins.2015.00467.
[41] M. Lauritzen, L. Gold, Brain Function and Neurophysiological Correlates of Signals Used in Functional Neuroimaging, The Journal of Neuroscience. 23 (2003) 3972–3980. https://doi.org/10.1523/JNEUROSCI.23-10-03972.2003.
[42] M. Zhao, H. Ma, M. Suh, T.H. Schwartz, Spatiotemporal Dynamics of Perfusion and Oximetry during Ictal Discharges in the Rat Neocortex, Journal of Neuroscience. 29 (2009) 2814–2823. https://doi.org/10.1523/JNEUROSCI.4667-08.2009.
[43] S. Reddy, I. Younus, V. Sridhar, D. Reddy, Neuroimaging Biomarkers of Experimental Epileptogenesis and Refractory Epilepsy, Int J Mol Sci. 20 (2019) 220. https://doi.org/10.3390/ijms20010220.
[44] M.M. Mirrione, W.K. Schiffer, M. Siddiq, S.L. Dewey, S.E. Tsirka, PET imaging of glucose metabolism in a mouse model of temporal lobe epilepsy, Synapse. 59 (2006) 119–121. https://doi.org/10.1002/syn.20216.
[45] H.I. Kornblum, D.M. Araujo, A.J. Annala, K.J. Tatsukawa, M.E. Phelps, S.R. Cherry, In vivo imaging of neuronal activation and plasticity in the rat brain by high resolution positron emission tomography (microPET), Nat Biotechnol. 18 (2000) 655–660. https://doi.org/10.1038/76509.
[46] E. Fernandes, A. Ledo, R.M. Barbosa, Design and Evaluation of a Lactate Microbiosensor: Toward Multianalyte Monitoring of Neurometabolic Markers In Vivo in the Brain, Molecules. 27 (2022) 514. https://doi.org/10.3390/molecules27020514.
[47] J.M. Rho, Inhibition of Lactate Dehydrogenase to Treat Epilepsy, New England Journal of Medicine. 373 (2015) 187–189. https://doi.org/10.1056/NEJMcibr1503558.
[48] N. Sada, S. Suto, M. Suzuki, S. Usui, T. Inoue, Upregulation of lactate dehydrogenase A in a chronic model of temporal lobe epilepsy, Epilepsia. 61 (2020). https://doi.org/10.1111/epi.16488.
[49] L. Zhou, H. Hou, H. Wei, L. Yao, L. Sun, P. Yu, B. Su, L. Mao, In Vivo Monitoring of Oxygen in Rat Brain by Carbon Fiber Microelectrode Modified with Antifouling Nanoporous Membrane, Anal Chem. 91 (2019) 3645–3651. https://doi.org/10.1021/acs.analchem.8b05658.
[50] A. Ledo, C.F. Lourenço, J. Laranjinha, C.M.A. Brett, G.A. Gerhardt, R.M. Barbosa, Ceramic-Based Multisite Platinum Microelectrode Arrays: Morphological Characteristics and Electrochemical Performance for Extracellular Oxygen Measurements in Brain Tissue, Anal Chem. 89 (2017) 1674–1683. https://doi.org/10.1021/acs.analchem.6b03772.
[51] C. Zhang, S. Bélanger, P. Pouliot, F. Lesage, Measurement of Local Partial Pressure of Oxygen in the Brain Tissue under Normoxia and Epilepsy with

Phosphorescence Lifetime Microscopy, PLoS One. 10 (2015) e0135536. https://doi.org/10.1371/journal.pone.0135536.
[52] M. Patel, L.-P. Liang, H. Hou, B.B. Williams, M. Kmiec, H.M. Swartz, J.P. Fessel, L.J. Roberts, Seizure-induced formation of isofurans: novel products of lipid peroxidation whose formation is positively modulated by oxygen tension, J Neurochem. 0 (2007) 071024001227006-??? https://doi.org/10.1111/j.1471-4159.2007.04974.x.
[53] J.F. Dunn, H.M. Swartz, In vivo electron paramagnetic resonance oximetry with particulate materials, Methods. 30 (2003) 159–166. https://doi.org/10.1016/S1046-2023(03)00077-X.
[54] K. Bartlett, M. Saka, M. Jones, Polarographic Electrode Measures of Cerebral Tissue Oxygenation: Implications for Functional Brain Imaging, Sensors. 8 (2008) 7649–7670. https://doi.org/10.3390/s8127649.
[55] C. Xu, F. Wu, P. Yu, L. Mao, *In Vivo* Electrochemical Sensors for Neurochemicals: Recent Update, ACS Sens. 4 (2019) 3102–3118. https://doi.org/10.1021/acssensors.9b01713.
[56] O. Ndubuizu, J.C. LaManna, Brain Tissue Oxygen Concentration Measurements, Antioxid Redox Signal. 9 (2007) 1207–1220. https://doi.org/10.1089/ars.2007.1634.
[57] P.T. Kissinger, W.R. Heineman, Cyclic voltammetry, J Chem Educ. 60 (1983) 702. https://doi.org/10.1021/ed060p702.
[58] B. Zhang, M.L.A. v. Heien, M.F. Santillo, L. Mellander, A.G. Ewing, Temporal Resolution in Electrochemical Imaging on Single PC12 Cells Using Amperometry and Voltammetry at Microelectrode Arrays, Anal Chem. 83 (2011) 571–577. https://doi.org/10.1021/ac102502g.
[59] G. Jobst, G. Urban, A. Jachimowicz, F. Kohl, O. Tilado, I. Lettenbichler, G. Nauer, Thin-film Clark-type oxygen sensor based on novel polymer membrane systems for in vivo and biosensor applications, Biosens Bioelectron. 8 (1993) 123–128. https://doi.org/10.1016/0956-5663(93)85024-I.
[60] J. Wu, H. Yang, Platinum-Based Oxygen Reduction Electrocatalysts, Acc Chem Res. 46 (2013) 1848–1857. https://doi.org/10.1021/ar300359w.
[61] E. Yeager, Electrocatalysts for O2 reduction, Electrochim Acta. 29 (1984) 1527–1537. https://doi.org/10.1016/0013-4686(84)85006-9.
[62] J. Sheng, Y. Li, Applications of Carbon Nanotubes in Oxygen Electrocatalytic Reactions, ACS Appl Mater Interfaces. 14 (2022) 20455–20462. https://doi.org/10.1021/acsami.1c08104.
[63] M. Cheng, G. Zhu, F. Zhang, W. Tang, S. Jianping, J. Yang, L. Zhu, A review of flexible force sensors for human health monitoring, J Adv Res. 26 (2020) 53–68. https://doi.org/10.1016/j.jare.2020.07.001.
[64] L. Issman, P.A. Kloza, J. Terrones Portas, B. Collins, A. Pendashteh, M. Pick, J.J. Vilatela, J.A. Elliott, A. Boies, Highly Oriented Direct-Spun Carbon Nanotube Textiles Aligned by In Situ Radio-Frequency Fields, ACS Nano. 16 (2022) 9583–9597. https://doi.org/10.1021/acsnano.2c02875.
[65] Q.W. Li, Y. Li, X.F. Zhang, S.B. Chikkannanavar, Y.H. Zhao, A.M. Dangelewicz, L.X. Zheng, S.K. Doorn, Q.X. Jia, D.E. Peterson, P.N. Arendt, Y.T. Zhu, Structure-Dependent Electrical Properties of Carbon Nanotube Fibers, Advanced Materials. 19 (2007) 3358–3363. https://doi.org/10.1002/adma.200602966.

[66] X. Zhao, X. Lu, W.T.Y. Tze, P. Wang, A single carbon fiber microelectrode with branching carbon nanotubes for bioelectrochemical processes, Biosens Bioelectron. 25 (2010) 2343–2350. https://doi.org/10.1016/j.bios.2010.03.030.
[67] Y. Wang, Q. Li, S. Hu, A multiwall carbon nanotubes film-modified carbon fiber ultramicroelectrode for the determination of nitric oxide radical in liver mitochondria, Bioelectrochemistry. 65 (2005) 135–142. https://doi.org/10.1016/j.bioelechem.2004.10.002.
[68] R.M. Santos, J. Laranjinha, R.M. Barbosa, A. Sirota, Simultaneous measurement of cholinergic tone and neuronal network dynamics in vivo in the rat brain using a novel choline oxidase based electrochemical biosensor, Biosens Bioelectron. 69 (2015) 83–94. https://doi.org/10.1016/j.bios.2015.02.003.
[69] L. Kandratavicius, P.A. Balista, C. Lopes-Aguiar, R.N. Ruggiero, E.H. Umeoka, N. Garcia-Cairasco, L.S. Bueno-Junior, J.P. Leite, Animal models of epilepsy: use and limitations., Neuropsychiatr Dis Treat. 10 (2014) 1693–705. https://doi.org/10.2147/NDT.S50371.
[70] J.P. Leite, N. Garcia-Cairasco, E.A. Cavalheiro, New insights from the use of pilocarpine and kainate models, Epilepsy Res. 50 (2002) 93–103. https://doi.org/10.1016/S0920-1211(02)00072-4.
[71] M. Lévesque, M. Avoli, C. Bernard, Animal models of temporal lobe epilepsy following systemic chemoconvulsant administration, J Neurosci Methods. 260 (2016) 45–52. https://doi.org/10.1016/j.jneumeth.2015.03.009.
[72] A. Gonzalez-Sulser, J. Wang, G.K. Motamedi, M. Avoli, S. Vicini, R. Dzakpasu, The 4-aminopyridine in vitro epilepsy model analyzed with a perforated multi-electrode array, Neuropharmacology. 60 (2011) 1142–1153. https://doi.org/10.1016/j.neuropharm.2010.10.007.
[73] A.M. King, N.B. Menke, K.D. Katz, A.F. Pizon, 4-Aminopyridine Toxicity: a Case Report and Review of the Literature, Journal of Medical Toxicology. 8 (2012) 314–321. https://doi.org/10.1007/s13181-012-0248-9.
[74] M. Avoli, M. D'Antuono, J. Louvel, R. Köhling, G. Biagini, R. Pumain, G. D'Arcangelo, V. Tancredi, Network and pharmacological mechanisms leading to epileptiform synchronization in the limbic system in vitro, Prog Neurobiol. 68 (2002) 167–207. https://doi.org/10.1016/S0301-0082(02)00077-1.
[75] A.E. Watts, J.G.R. Jefferys, Effects of carbamazepine and baclofen on 4-aminopyridine-induced epileptic activity in rat hippocampal slices, Br J Pharmacol. 108 (1993) 819–823. https://doi.org/10.1111/j.1476-5381.1993.tb12884.x.
[76] J.S. Farrell, I. Gaxiola-Valdez, M.D. Wolff, L.S. David, H.I. Dika, B.L. Geeraert, X. Rachel Wang, S. Singh, S.C. Spanswick, J.F. Dunn, M.C. Antle, P. Federico, G.C. Teskey, Postictal behavioural impairments are due to a severe prolonged hypoperfusion/hypoxia event that is COX-2 dependent, Elife. 5 (2016). https://doi.org/10.7554/eLife.19352.
[77] R.L. Kow, K. Jiang, A. v. Naydenov, J.H. Le, N. Stella, N.M. Nathanson, Modulation of Pilocarpine-Induced Seizures by Cannabinoid Receptor 1, PLoS One. 9 (2014) e95922. https://doi.org/10.1371/journal.pone.0095922.
[78] M. Lévesque, M. Avoli, The kainic acid model of temporal lobe epilepsy, Neurosci Biobehav Rev. 37 (2013) 2887–2899. https://doi.org/10.1016/j.neubiorev.2013.10.011.

[79] A. Semyanov, D.M. Kullmann, Kainate receptor-dependent axonal depolarization and action potential initiation in interneurons, Nat Neurosci. 4 (2001) 718–723. https://doi.org/10.1038/89506.
[80] B. Söderfeldt, H. Kalimo, Y. Olsson, B.K. Siesjö, Bicuculline-induced epileptic brain injury, Acta Neuropathol. 62 (1983) 87–95. https://doi.org/10.1007/BF00684924.
[81] T. Shimada, K. Yamagata, Pentylenetetrazole-Induced Kindling Mouse Model, Journal of Visualized Experiments. (2018). https://doi.org/10.3791/56573.
[82] H. Straub, R. Köhling, E.-J. Speckmann, Picrotoxin-induced epileptic activity in hippocampal and neocortical slices (guinea pig): suppression by organic calcium channel blockers, Brain Res. 658 (1994) 119–126. https://doi.org/10.1016/S0006-8993(09)90017-8.
[83] P. Gloor, L.F. Quesney, H. Zumstein, Pathophysiology of generalized penicillin epilepsy in the cat: the role of cortical and subcortical structures. II. Topical application of penicillin to the cerebral cortex and to subcortical structures, Electroencephalogr Clin Neurophysiol. 43 (1977) 79–94. https://doi.org/10.1016/0013-4694(77)90198-5.
[84] P. Gloor, R.G. Fariello, Generalized epilepsy: some of its cellular mechanisms differ from those of focal epilepsy, Trends Neurosci. 11 (1988) 63–68. https://doi.org/10.1016/0166-2236(88)90166-X.
[85] R. Sander, Compilation of Henry's law constants (version 4.0) for water as solvent, Atmos Chem Phys. 15 (2015) 4399–4981. https://doi.org/10.5194/acp-15-4399-2015.
[86] R.M. Santos, C.F. Lourenço, A.P. Piedade, R. Andrews, F. Pomerleau, P. Huettl, G.A. Gerhardt, J. Laranjinha, R.M. Barbosa, A comparative study of carbon fiber-based microelectrodes for the measurement of nitric oxide in brain tissue, Biosens Bioelectron. 24 (2008) 704–709. https://doi.org/10.1016/j.bios.2008.06.034.
[87] A. Ledo, E. Fernandes, J.E. Quintero, G.A. Gerhardt, R.M. Barbosa, Electrochemical Evaluation of a Multi-Site Clinical Depth Recording Electrode for Monitoring Cerebral Tissue Oxygen, Micromachines (Basel). 11 (2020) 632. https://doi.org/10.3390/mi11070632.
[88] E. Bernalte, C. Foster, D. Brownson, M. Mosna, G. Smith, C. Banks, Pencil It in: Exploring the Feasibility of Hand-Drawn Pencil Electrochemical Sensors and Their Direct Comparison to Screen-Printed Electrodes, Biosensors (Basel). 6 (2016) 45. https://doi.org/10.3390/bios6030045.
[89] C.J. Meunier, J.D. Denison, G.S. McCarty, L.A. Sombers, Interpreting Dynamic Interfacial Changes at Carbon Fiber Microelectrodes Using Electrochemical Impedance Spectroscopy, Langmuir. 36 (2020) 4214–4223. https://doi.org/10.1021/acs.langmuir.9b03941.
[90] sensitivity in metrology and analytical chemistry, A, in: The IUPAC Compendium of Chemical Terminology, International Union of Pure and Applied Chemistry (IUPAC), Research Triangle Park, NC, 2014. https://doi.org/10.1351/goldbook.S05606.
[91] R.M. Barbosa, C.F. Lourenço, R.M. Santos, F. Pomerleau, P. Huettl, G.A. Gerhardt, J. Laranjinha, In Vivo Real-Time Measurement of Nitric Oxide in Anesthetized Rat Brain, in: 2008: pp. 351–367. https://doi.org/10.1016/S0076-6879(08)01220-2.

[92] Bondarenko A S and Ragoisha G A 2005 Progress in Chemometrics Research ed A. L. Pomerantsev (New York: Nova Science Publishers) 89-102 the program is available online at http://www.abc.chemistry.bsu.by/vi/analyser/), (n.d.).
[93] Bard A. J., Faulkner L.R.: Electrochemical Methods: Fundamentals and Applications (2 ed.) (2000) Wiley. ISBN 978-0-471-04372-0., n.d.
[94] Y. Hu, G.S. Wilson, Rapid Changes in Local Extracellular Rat Brain Glucose Observed with an In Vivo Glucose Sensor, J Neurochem. 68 (2002) 1745–1752. https://doi.org/10.1046/j.1471-4159.1997.68041745.x.
[95] T. Back, K. Kohno, K.-A. Hossmann, Cortical Negative DC Deflections following Middle Cerebral Artery Occlusion and KCl-Induced Spreading Depression: Effect on Blood Flow, Tissue Oxygenation, and Electroencephalogram, Journal of Cerebral Blood Flow & Metabolism. 14 (1994) 12–19. https://doi.org/10.1038/jcbfm.1994.3.
[96] L. Douw, E. van Dellen, M. de Groot, J.J. Heimans, M. Klein, C.J. Stam, J.C. Reijneveld, Epilepsy is related to theta band brain connectivity and network topology in brain tumor patients, BMC Neurosci. 11 (2010) 103. https://doi.org/10.1186/1471-2202-11-103.
[97] D. Budai, Carbon Fiber-based Microelectrodes and Microbiosensors, in: Intelligent and Biosensors, InTech, 2010. https://doi.org/10.5772/7158.
[98] N.R. Ferreira, R.M. Santos, J. Laranjinha, R.M. Barbosa, Real Time In Vivo Measurement of Ascorbate in the Brain Using Carbon Nanotube-Modified Microelectrodes, Electroanalysis. 25 (2013) 1757–1763. https://doi.org/10.1002/elan.201300053.
[99] F. Yusoff, N. Mohamed, A. Aziz, S.A. Ghani, Electrocatalytic Reduction of Oxygen at Perovskite (BSCF)-MWCNT Composite Electrodes, Materials Sciences and Applications. 05 (2014) 199–211. https://doi.org/10.4236/msa.2014.54025.
[100] C.E. Cava, R.V. Salvatierra, D.C.B. Alves, A.S. Ferlauto, A.J.G. Zarbin, L.S. Roman, Self-assembled films of multi-wall carbon nanotubes used in gas sensors to increase the sensitivity limit for oxygen detection, Carbon N Y. 50 (2012) 1953–1958. https://doi.org/10.1016/j.carbon.2011.12.048.
[101] F. Vitale, S.R. Summerson, B. Aazhang, C. Kemere, M. Pasquali, Neural Stimulation and Recording with Bidirectional, Soft Carbon Nanotube Fiber Microelectrodes, ACS Nano. 9 (2015) 4465–4474. https://doi.org/10.1021/acsnano.5b01060.
[102] Z. Deng, L. Zhao, H. Mu, L. Jiang, W. Xi, X. Xu, W. Zheng, High selective property of gelatin/MWCNTs functionalized carbon fiber microelectrode: Toward real-time monitoring of ascorbate, Journal of Electroanalytical Chemistry. 914 (2022) 116315. https://doi.org/10.1016/j.jelechem.2022.116315.
[103] K. Rajavel, M. Lalitha, J.K. Radhakrishnan, L. Senthilkumar, R.T. Rajendra Kumar, Multiwalled Carbon Nanotube Oxygen Sensor: Enhanced Oxygen Sensitivity at Room Temperature and Mechanism of Sensing, ACS Appl Mater Interfaces. 7 (2015) 23857–23865. https://doi.org/10.1021/acsami.5b04869.
[104] C. Yang, E. Trikantzopoulos, C.B. Jacobs, B.J. Venton, Evaluation of carbon nanotube fiber microelectrodes for neurotransmitter detection: Correlation of electrochemical performance and surface properties, Anal Chim Acta. 965 (2017) 1–8. https://doi.org/10.1016/j.aca.2017.01.039.

[105] A.E. Ross, B.J. Venton, Nafion–CNT coated carbon-fiber microelectrodes for enhanced detection of adenosine, Analyst. 137 (2012) 3045. https://doi.org/10.1039/c2an35297d.
[106] C. Yang, Y. Wang, C.B. Jacobs, I.N. Ivanov, B.J. Venton, O 2 Plasma Etching and Antistatic Gun Surface Modifications for CNT Yarn Microelectrode Improve Sensitivity and Antifouling Properties, Anal Chem. 89 (2017) 5605–5611. https://doi.org/10.1021/acs.analchem.7b00785.
[107] S.B. Hočevar, J. Wang, R.P. Deo, M. Musameh, B. Ogorevc, Carbon Nanotube Modified Microelectrode for Enhanced Voltammetric Detection of Dopamine in the Presence of Ascorbate, Electroanalysis. 17 (2005) 417–422. https://doi.org/10.1002/elan.200403175.
[108] B.M. Ances, Coupling of Changes in Cerebral Blood Flow with Neural Activity: What Must Initially Dip Must Come Back Up, Journal of Cerebral Blood Flow & Metabolism. 24 (2004) 1–6. https://doi.org/10.1097/01.WCB.0000103920.96801.12.